We would like to thank the reviewers and editor for all the useful feedback and suggestions. We have made significant additions to our manuscript in response to the feedback, and feel this has greatly improved the paper. Most notably, we have added a section to discuss the water vapor correction, and added figures to support this discussion. We have added more uncertainty analysis to address this important concern as well. Further, we have added some figures highlighting the impact of using mass flow control and illustrating what individual calibrations look like for our in-flight system. We address each comment in a line-by-line fashion below, and changes are highlighted in the updated document.

J. R. Pitt:
It has now become well-known in the trace gas measurement community that analysers employing Tunable Infrared Laser Direct Absorption Spectroscopy (TILDAS) techniques on aircraft can exhibit a strong sensitivity to changes in cabin pressure. This is currently a major limitation to the utility of these instruments for airborne sampling, as operators either have to accept large altitude-dependent biases in their final dataset or very low duty cycles (as the instrument must be recalibrated at each altitude). Many important trace gas species (e.g. N2O and C2H6) have much stronger absorption lines in the mid-infrared than the near-IR; whilst cavity-based measurement techniques for these species have developed significantly in recent years, TILDAS is still the most commonly used technique for measuring many trace gases in the mid-IR. Therefore improving the accuracy and duty cycle of TILDAS instruments during aircraft sampling is important if we are to improve our understanding of key greenhouse and pollutant gases.

This paper presents a novel calibration strategy to tackle this issue, resulting in greatly reduced altitude-dependent biases with a 90% duty cycle. The switch to controlling mass flow instead of pressure is a clever idea, removing issues associated with pressure instability during the sample-calibration transition. The method employed here will certainly be of great interest to anyone currently operating TILDAS analysers on aircraft, but it also provides the potential for reducing biases and/or increasing the duty cycle for other airborne instrumentation. I recommend its publication in AMT, but I have the following suggestions for minor revisions.

The water broadening correction is mentioned at the end of section 2.1. Did you determine the water broadening to air broadening ratio yourself experimentally? If so perhaps state this explicitly because at the moment it makes it seem like TDLWintel does this automatically without user intervention (unless Aerodyne tested your instrument before sending it to you – in which case mention this because as far as I'm aware it isn't what they don't usually do). Assuming you determined the coefficients yourself, could you add a brief outline of the general approach taken (e.g. H2O injection/dew point generator/etc. . .) and the uncertainties associated with it please? The uncertainty associated with this water vapour correction is often on the same order as the other uncertainties so it's important to consider it.

Thank you for raising this point – this is of great importance to accurate trace gas observations and we have added a section discussing this. We now describe the water broadening coefficients, our determination of the values, and the associated uncertainties, and we have added a figure showing the effect of the correction as a function of water vapor. We used a moist filter similar to Lebegue et al. 2016, and sampled a mixture of wet and dry tank air which we then reanalyzed to find the proper coefficients. Table 1 has also been updated to include these uncertainties. We also note that in adding this discussion we realized the proper water broadening coefficients were not consistently applied to the data presented initially. We have corrected this oversight for this dataset in all the data and figures presented in the revision.

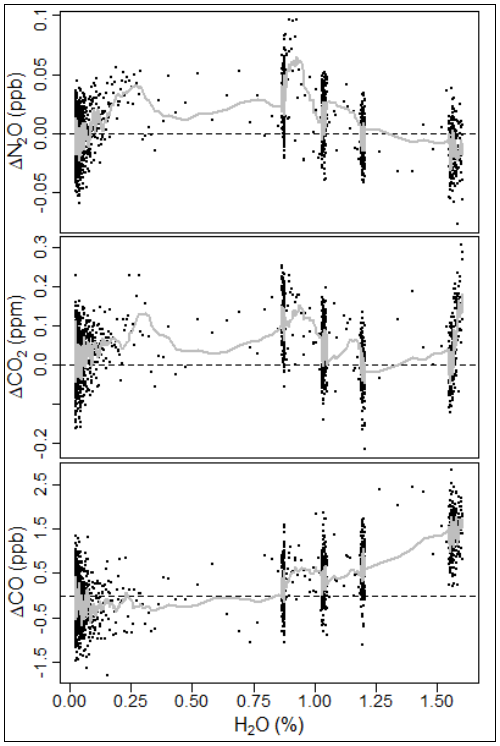

Section 2.3 is presented in a rather confusing way. I think this is largely because the use of two in-flight calibration gases is introduced here, but the fact that one of them is used as a check gas is not mentioned until section 4.1. It wasn't until I got to this point much later in the text that I fully understood what was going on (e.g. why the long-term drift in instrument slope needed quantifying in the lab) – it would be much better if it was explicitly stated in section 2.3 that a single-point calibration strategy with an additional check gas was used in-flight. Additionally, the term "linearity" is used in a way here that isn't intuitive to me. I would stick to using the word "slope" throughout (or "gain" if an alternative is needed), as what is being tested here is the extent to which the instrument slope drifts with time. In my mind instrument linearity is the extent to which the linear fit used here is applicable, not whether the coefficients are drifting with time. To assess linearity three cylinders with different mole fractions are therefore needed. This hasn't been done here, but these instruments are known to have a good linear response so it's probably safe to assume non-linearity is a small component of the uncertainty budget.

We have updated Section 2.3 to clarify this point as suggested. We have also changed the use of "linearity" to the more appropriate "slope" throughout.

Section 3.2: having had many discussions with Aerodyne about this following on from our 2014/15 campaigns, I am fairly certain that the main source of the large gradients in mole fraction you see during profiles is indeed an optical fringe (or possibly multiple fringes), activated by the change in cabin pressure. However we do also see artefacts in the measurements associated with aircraft acceleration as well – for us these manifest themselves as much smaller-timescale features which would not be captured by the calibration strategy here.

Optical fringes are likely the dominant component. Acceleration-induced artifacts can have very short duration (g-force), and not be well-captured by the method here. They can also have a longer duration (e.g. large engine pull for the duration of a climb possibly impacting instrument via electrical feedbacks), and these would be captured. As shown in the paper, longer-duration features dominate our artifact and thus are the focus of improvements.

We have added clarification to the end of first paragraph in section 3.2 "Artifacts that occur on shorter time-frames, such as induced by a short duration turbulence event, will not be corrected with this method."

Section 4: our experience is that there is significant flight-to-flight variability in the cabin pressure artefact, making it impossible to apply a single correction throughout a campaign. This is because, while the FSR of the fringe at ground level stays constant, its initial phase is variable and unpredictable. We did experiment with doing two deep profiles at the beginning and end of a flight on tank air to try and calibrate out this effect, but the drift during the flight resulted in a large

uncertainty and we abandoned this approach. Essentially I'm not convinced that this effect is repeatable enough to take data from a single null flight and use it to correct other flights, so I'd probably remove that paragraph (unless you have evidence to the contrary). The method you've developed here seems far superior to any that could be developed from the null test results.

We agree that our method is an improvement on attempting a single cabin pressure artifact correction. We've modified the text in Section 4 as outlined below to clarify.

"Given the repeatable, smooth nature of the cabin pressure artifact, it *would seem* possible to use just the cabin pressure data to empirically correct for the artifact, without running frequent calibrations. This method *would not* account for long-term spectral drift however or traceability, *and relies on the assumption that the cabin pressure artifact will be stable and repeatable*. *These weaknesses compromise such an approach.*"

I'd be interested to know more about the suspected contamination which has resulted in the 0.6 ppm CO2 offset between the Picarro and the FCHAOS systems. Have you been able to identify which of the systems the contamination is associated with? Reading the manuscript I initially assumed that it was the FCHAOS regulator/tubing that was under suspicion, but it would be good to make this explicit, or if it is still unknown which instrument was contaminated to state that. Was there any change to the setup in future campaigns where this offset was not observed? The regulator and tubing used for the FCHAOS here are pretty standard, so if there are contamination effects associated with either it would be good to know about them! Or is the theory that the cylinder itself became contaminated (e.g. due to a mistake during regulator flushing)? Surely in that case you would also expect to see the offset in the check cylinder data in Figure 8? In the first half of the campaign (before the cylinder switch) there may be a sign of a negative bias in CO2, but there doesn't appear to be a corresponding positive bias in the second half, so this doesn't really tally with a single cylinder contamination. Also in that case you'd expect the Picarro bias only to be present in one half of the campaign but I can't see any evidence of this in Figure 7. If you haven't made any further progress in diagnosing this then no worries, but it would be good to include any extra details you do have.

We appreciate your interest in this cause. We have gone back through in further detail trying to isolate a potential cause, but still are left with a somewhat unsatisfactory suspicion of contamination. We have modified the text in Section 4 slightly in accordance with this. We also add the discussion here to further highlight the importance of the water vapor correction you raised earlier, noting that residual water vapor errors (in either the FCHAOS or Picarro systems) could contribution to perceived biases.

The fact you don't see the same effect on the H2O measurements is very interesting, but I can't quite see this from the plots included here. Could you add another column in Fig. 4 showing H2O please? I know the tanks were dry but you are assuming (in my view reasonably) that the artefact is a simple offset shift so it shouldn't matter what the absolute value of the H2O mole fraction is – even if it is completely dry I'd expect the fringing to affect this zero-offset reading. I don't doubt your word here, but the explanations offered as to why the fringe would affect H2O less don't really make sense to me either so I could do with a bit more detail on these. Surely the fringe amplitude will increase with laser intensity, if anything making the problem worse? The relevant signal-to-noise here is the strength of the absorption peak (not the laser intensity) relative to the fringe amplitude. If the H2O line in question is the one at ~2227.5 cm-1 then this tends to be a weak feature relative to the N2O and CO2 lines, so again I would have thought that H2O would be more affected by the fringe. I'm also not sure why having a line frequency of ~2227.5 cm-1 compared to the CO2 line at ~2227.6 cm-1 (for instance) would reduce the fringe interference. It is definitely true that a very wide absorption feature would suffer less from a fringe with a small FSR, but I don't think the H2O line is wider than the other peaks here? Sorry to labour the point on this, but the fact that you don't observe the fringe effect on the H2O measurement could be a really useful piece of information in trying to further mitigate this issue, so I'm keen to better establish the cause of it.

Thank you for digging into this question further. We have updated Section 4 when discussing comparisons between FCHAOS and the Picarro, and added the figure below to show the water vapor during the null test profiles as well as difference between FCHAOS and Picarro measured water vapor as a function of altitude. The long equilibration time for water vapor makes it difficult for us to see an altitude artifact if it is present. One null test profile suggests there may be a ~60 ppm water vapor vertical sensitivity, but it is difficult to clearly establish. In the comparison with the Picarro we see no evidence of any vertical dependency of water vapor, though a dependency of 10s of ppm would be hidden within the respective instruments noise. We have updated the text to include this more nuanced discussion.

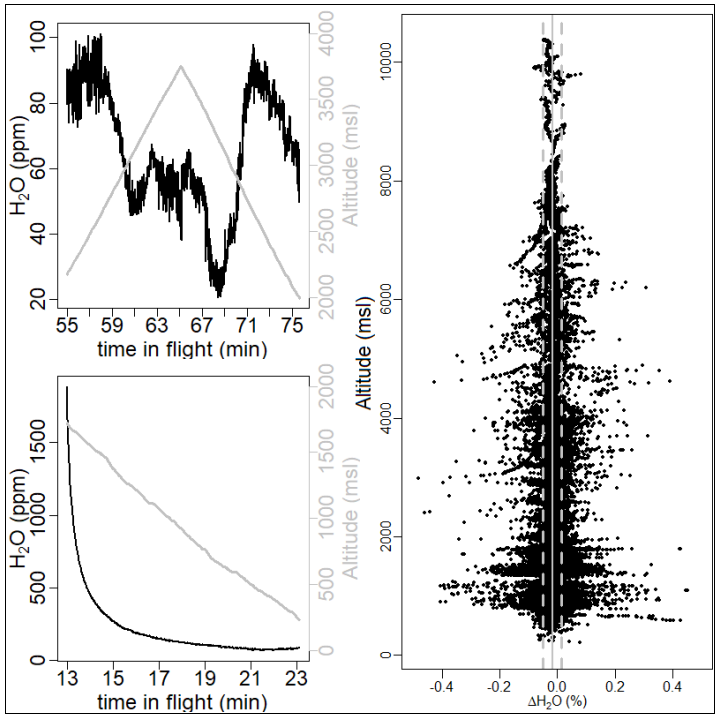

Section 5: Could you put details of the altitude and variability in altitude during the runs in here please? I assume it was essentially performed at a single level but if so it would be good to be clear about this just so the reader knows there are no vertical gradients convolved in here.

We have updated the text with the altitude values, affirming that the transects were at relatively constant altitude.

Specific points:

P3 L2 – Minor point but the LGR FGGA in O'Shea et al. is a near-IR instrument

Thank you for catching that, we have updated the text for accuracy.

P3 L26 – Typo: missing space

Corrected.

P5 L18 – ". . .within our 1 Hz precision. . ."

Corrected.

P7 L9 – ". . .at the same flow-rate. . ."

Corrected.

P7 L12 – What interpolation technique was used?

Forsythe, Malcolm, and Moler (FMM) cubic spline interpolation, we have added this to the text.

P8 L8 – ". . .within our 1 Hz precision."

Corrected.

Anonymous Referee #2:

This work presents airborne data of an in-situ QCL absorption spectrometer measuring greenhouse gases N2O, CO2, CO, and H2O with a commercial Aerodyne spectrometer. Such instruments tend to show strong drifts due to changing pressure and/or temperature inside the aircraft cabin. This holds particular during ascent and descent and for unpressurized platforms.

To reduce the effect of the drift, the authors apply a calibration system, which is new according to the authors - the frequent calibration high performance airborne observation system (FCHAOS). Basically the absorption cell of the IR-spectrometer is frequently flushed with a high flow of calibration cylinders with ambient mixing ratios of the target gases tracable to the NOAA WMO scale. The authors apply a duty cycle of 120 s and purge the cell for 10 s with additional 5 s latency before measuring. The output frequency is 1 Hz. The authors show, that by applying this calibration procedure the effect of the drift is accounted for. In-flight comparisons with a PICARRO CRDS system confirms this. The correction is shown for N2O data during a research flight and demonstrates the effect of the procedure.

The paper is well written and documents the calibration procedure allowing to reduce instrumental drift particularly during ascent and descent. I fully acknowledge a clear documentation of instrumental performance and data processing. However, I can't see the novelty of the approach. Fast flow and frequent short calibration with subsequent linear drift correction is basically, what has been applied here. Note, that 1.5 slpm are not novel (e.g. Korrmann et al., 2005 used 1-1.5 slpm at 56 hPa, cell < 0.5 l) as well as linear drift correction is standard.

If the authors could show, that the regulation of mass flow (MFC) upstream the cell (and downstream the cal switch valve) is the key to guarantee short calibration times by reducing pressure pulses (as suggested in the conclusions) I would see a potential new aspect. For this they should provide e.g. comparisons between pressure and flow controlled approaches (see below). It is not shown, why a pressure controlled system should not have the same performance.

As the paper currently stands, it is a well documented calibration procedure of a commercial instrument with standard methods. Therefore I don't see the paper in AMT in its current form.

We respectfully disagree with the perspective that this paper only presents a calibration procedure (that is not novel to this reviewer) and thus is not worthy of publication in AMT. This criticism is founded on two underlying perspectives: 1) That the only new value of this paper is the presentation of a new calibration method & 2) the calibration method is not novel. We disagree with both perspectives. Firstly, the paper is not solely about a calibration method. This paper is the first presentation of this flight system and shows extensive validation with in-flight null tests and direct comparison with a Picarro. Even if the calibration approach was not novel, reporting the instrument performance and traceability with validation in such detail warrants publication on its own in AMT, and in fact is necessary for the community to have confidence in the data reported from this flight system, particularly considering the most similar flight system published cannot collect data during vertical profiles (Pitt et al. 2016). This is consistent with AMT standards and the expectation that papers "comprise the development, intercomparison, and validation of measurement instruments and techniques …" as evidenced by similar publications focused on intercomparison and validation (for example Santoni et al. 2014 & Pitt et al. 2016).

Regarding the calibration approach, it certainly can be considered a natural extension of previous calibration approaches. In spite of the apparent triviality of the approach, the combination of high flow rate, mass flow control and high frequency, short duration calibrations with near-ambient concentration cal gas has never been applied to other modern GHG systems. The most recent, state-of-the-science instrument paper on a flight QCLS N_2O system concluded they couldn't use data during vertical profiles (Pitt et al. 2016)—an important limitation for a flight instrument. While our approach may seem simple, we are able to achieve unprecedented in-flight performance in the face of dynamic environmental variables (cabin pressure, etc.), thus achieving a better duty cycle and more robust performance than any published flight N_2O system. We feel the overall approach is novel (and we note the other reviewers do as well), but even if the calibration method is felt to be simple, the extensive validation presented in the manuscript is new and necessary to document this systems performance.

Some of this concern may have arisen from lack of clarity in our writing. In response, we have made some changes to clarify that this is an extension of traditional methods and pinpoint the uniqueness of this approach (see abstract, intro, conclusion).

Also as requested, we have added a figure and discussion on the importance of the mass flow control approach (contrasting with the p-control setup) to more clearly illustrate some of the different elements/novelty of the setup.

This is outlined more below.

Main point:

If the use of an MFC is the key novelty this should be clearly documented in the analysis. The current Fig.1. and the text states, that three-way solenoid valves are used (p.4, l.16/17). In case of a calibration I expect a direct connection between the pressure transducer (calibration tank) and the MFC controlling the cell flow and thus a pressure pulse. The inlet line is probably closed during calibration. In case of switching from ambient to calibration I still expect a short pressure pulse perturbing MFC and cell pressure. This will probably stabilize after a few seconds since the MFC limits the flow, but I do not see the advantage or novelty over a calibration using overflow of calibration gas by flushing the inlet at ambient pressure, which has been applied since years to GHG measurements by TDLAS (or QCLAS).

Note, that many QCLAS or TDLAS systems often are calibrated by flushing the inlet line with higher flow rates than the cell flow. The calibration gas tube is directly connected to the inlet and thus ambient pressure solely via a t-connector in the inlet line. Calibration gas is just switched via an open/close valve. This ensures a minimum pressure perturbation of the cell due to the open connection of the calibration line to the inlet.

This has been established over a long time (e.g. Wienhold et al., 1998) and a potential advantage - if existing - via the proposed procedure in Gvakharia et al., should be documented.

Thank you for bringing this issue up. We are familiar with the excess flow, pressure control setup, and have flown such a system many times. We note one disadvantage of the excess flow setup is that it can lead to contamination of other instrument sampling for nearby inlets and thus is often not preferred (with a second weakness being larger cal gas consumption). Even with the excess flow setup, there will invariably be some pressure fluctuations in the cell when switching to calibration gas. Depending on the specifics of the pressure control setup, to achieve stable pressure control over the entire dynamic range sampled by the aircraft makes it a challenge to prevent any pressure blips when switching to calibration gas, though it may be possible. We show below here an example of a calibration with a pressure control setup (including excess flow) compared with the mass flow control. For our system, we have peak-to-peak fluctuations on the order of 0.8 Torr occur with the pressure control setup and transient pressure fluctuations that do not stabilize within 10s. With mass flow control, they are reduced to ~0.04 Torr, an order of magnitude smaller, and stabilize in much shorter times. We have added this figure and some related discussion to the manuscript in Section 2.2.

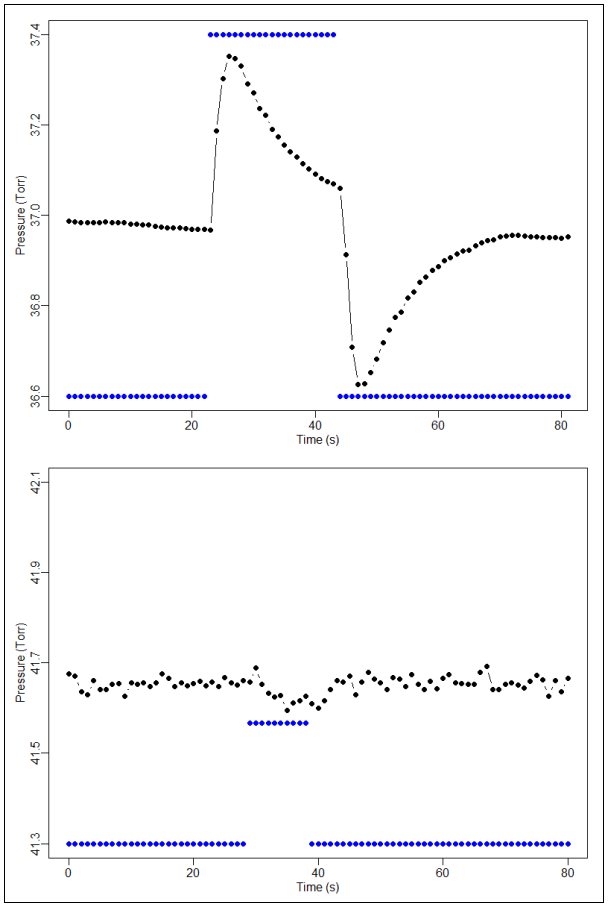

p.7. l.10-20: Would be good to see a highly resolved single calibration signal with individual data points and the cell pressure for a ground test and in-flight conditions at lower ambient pressure.

The plot below shows the calibration signal in flight, with ambient pressure around 730 mb. Similar to what was seen in the pressure plot above, the fluctuation in pressure is minimal when the valve changes. We have also added this figure to the manuscript in Section 3.2.

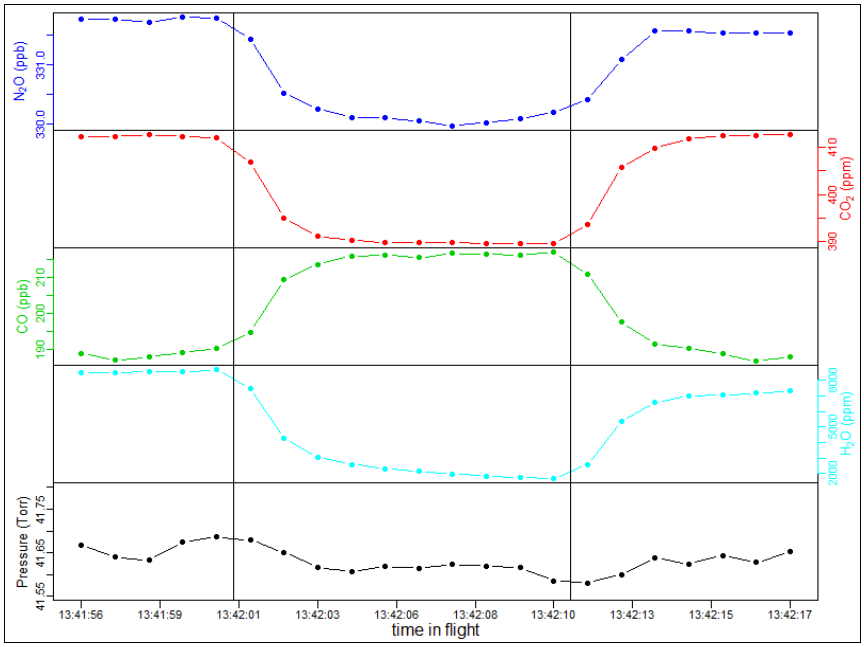

p.13, l.5: How do the respective Allan variance plots look like for the Nulltest? How do they compare to a lab test?

The top set of plots shows Allan variance for the 04/26 null test. The bottom set shows Allan variance plots for when gas was sampled on the ground (note tanks are dry so there is no H_2O). As is illustrated, the in-flight performance closely matches the ground performance, except noise is increased by a factor of 2. We have added text accordingly to make this point in Section 4.1.

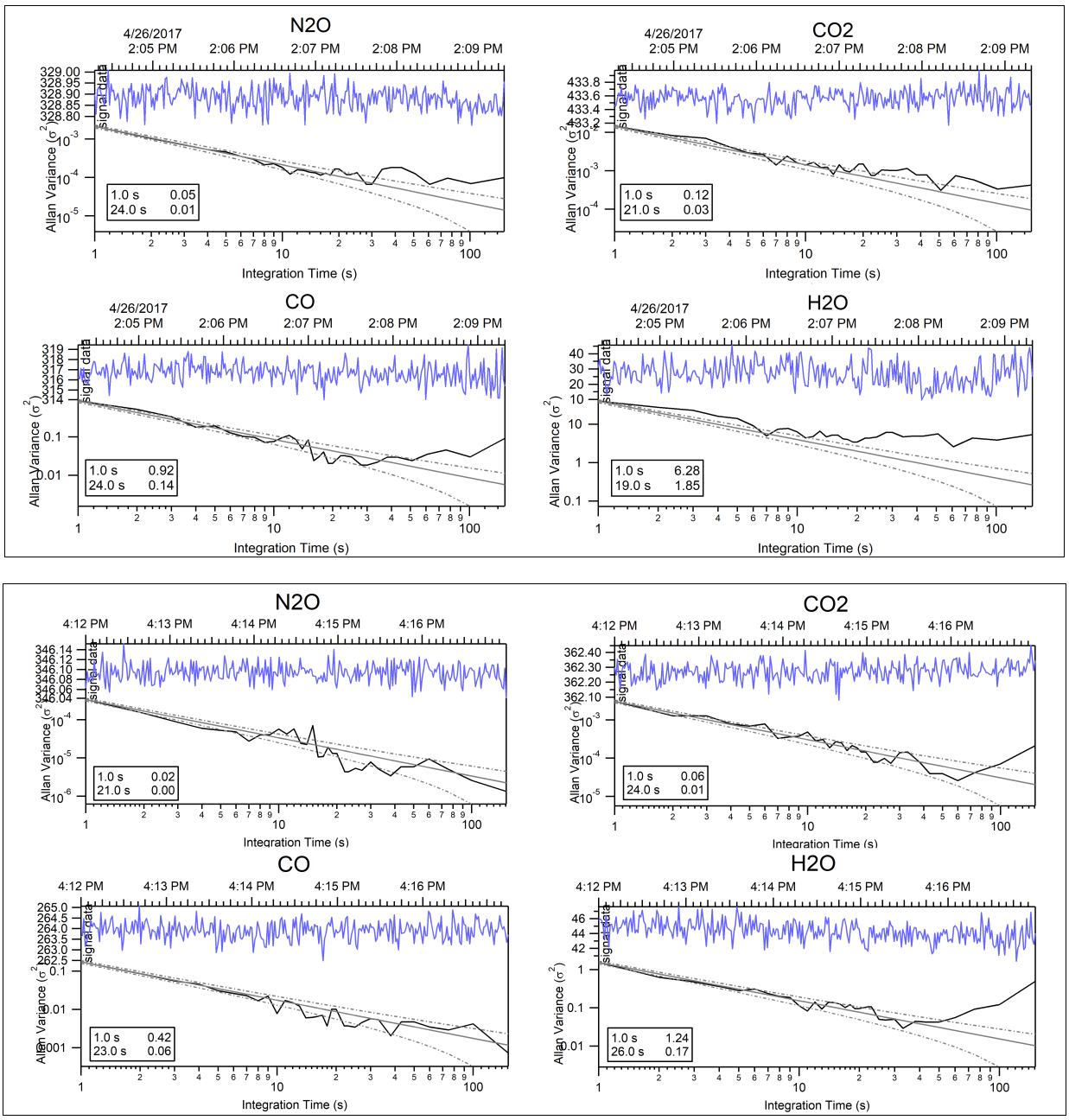

Fig.4: y-Axis: mixing ratio instead of concentration (also check the main text).

Thank you for the suggestion, we have updated Figure 4 as well as Figure 2 and checked the consistency of the main text.

Anonymous Referee #1:

The paper describes an airborne Tunable Infrared Laser Direct Absorption Spectroscopy (TILDAS) system for airborne atmospheric trace gas measurements. The focus is on a novel method to address cabin pressure induced changes in the measured mole fraction. The paper is well written, and fits well within the scope of AMT. However, a few issues listed below should be addressed before the paper can be recommended for publication.

Thank you for the useful feedback. We respond inline below.

General comments:

The potential impact of water vapour on the derived dry air mole fractions should be more elaborated. E.g. Pitt et al. (2016) mention a lack of long-term stability in the retrieval of H2O mole fractions using a similar instrument. Has the wet-dry correction been tested, and if so, what was the setup used for this? Also the difference of the Picarro G2301-f and FCHAOS water vapour measurements shows a standard deviation of 0.034%, which would correspond to uncertainties of 0.136 ppm CO2 (at 400 ppm) just due to dilution by H2O alone, more than the claimed precision of 0.1 ppm.

We address the water vapor correction in response to Dr. Pitt's review, so please refer to that above for more detail. We have tested the wet-dry correction and included information on the setup in Section 2.4. We have added new text and figures, regarding both the uncertainties due to water and any altitude-dependent sensitivity. This is an important issue so we have expanded our manuscript accordingly.

The 1σ difference of 340 ppm in water vapor between the two instruments would indeed cause a dilution uncertainty larger than the 1s precision of the instrument. We note that the precision is not where such an uncertainty should be described; instead potential water vapor correction errors impact the accuracy of the instrument and traceability to a known scale. Using the traceability standard we find an empirical check gas instrument accuracy of 0.30 ppm for CO_2 (in Table 1). The comparison with the Picarro shows variance of differences between the analyzers of 0.45 ppm for 1 s data. This slightly elevated value compared to the check gas approach may be related to the dilution, but may simply be variance in the Picarro. We have added this information to the manuscript in the Table to help clarify, and now have a total uncertainty value that accounts for the various sources of uncertainty, including the water vapor uncertainty impact.

Specific comments:

Fig. 1: In addition to the calibration tanks, there should also be a symbol for e.g. a pressure regulator of valve included.

Thank you for catching the omission, we have updated Figure 1.

Pg 4 Line 14: please clarify if there is excess flow escaping backward through the inlet when calibrating, or if calibration is performed by replacing the sample gas (solenoid valve closed to ambient, only open to filter/MFC). In the latter case I would expect slightly larger fluctuations in pressure within the inlet and filter,

There is no excess flow, the calibration does indeed switch directly from the inlet to the tanks with the solenoid valves to preventing potential contamination of other inlets and also not consume excess calibration gas. We have added a figure in Section 2.2 that shows the pressure variation when switching to a calibration gas in our system and clarified the text to explain our setup (replacement, no excess flow).

Testing and evaluation of a new airborne system for continuous N_2O, CO_2, CO, and H_2O measurements: the Frequent Calibration High-performance Airborne Observation System (FCHAOS)

Alexander Gvakharia[1], Eric A. Kort[1], Mackenzie L. Smith[1,2], and Stephen Conley[2]

[1]Climate and Space Sciences and Engineering, University of Michigan, Ann Arbor, Michigan, USA
[2]Scientific Aviation, Boulder, Colorado, USA

Correspondence to: Alexander Gvakharia (agvak@umich.edu)

Abstract. We present the development and assessment of a new flight system that uses a commercially available continuous-wave, tunable infrared laser direct absorption spectrometer to measure N_2O, CO_2, CO, and H_2O. When the commercial system is operated in an off-the-shelf manner, we find a clear cabin pressure/altitude dependency for N_2O, CO_2, and CO. The characteristics of this artifact make it difficult to reconcile with conventional calibration methods~~, so we~~. We present a novel procedure ~~employing~~ that extends upon traditional calibration approaches in a high-flow system with high-frequency, short-duration sampling of a known calibration gas of near-ambient concentration. This approach corrects for cabin pressure dependency as well as other sources of drift in the analyzer while maintaining a ~90% duty cycle for 1 Hz sampling. Assessment and validation of the flight system with both extensive in-flight calibrations and comparisons with other flight-proven sensors demonstrate the validity of this method. In-flight 1σ precision is estimated at 0.05 ppb, 0.10 ppm, 1.00 ppb, and 10 ppm for N_2O, CO_2, CO, and H_2O respectively, and traceability to WMO standards ~~is found to be 0.14 ppb, 0.34~~ (1σ) is 0.28 ppb, 0.33 ppm, and ~~2.33~~ 1.92 ppb for N_2O, CO_2, and CO. We show the system is capable of precise, accurate 1 Hz airborne observations of N_2O, CO_2, CO, and H_2O and highlight flight data illustrating the value of this analyzer for studying N_2O emissions on ~100 km spatial scales.

1 Introduction

Continuous, 1 Hz airborne observations of atmospheric greenhouse gases and pollutants provide essential information for direct quantification of emissions (Karion et al., 2015; Peischl et al., 2015; Smith et al., 2015; Kort et al., 2016), assessment of modeled representations of emissions and transport (Wofsy, 2011; O'Shea et al., 2014), and validation of remote sensing observations (Tanaka et al., 2016; Inoue et al., 2016; Frankenberg et al., 2016). Advances in the last decade have facilitated widespread, high-precision, high-accuracy continuous airborne observations of CH_4, CO_2, CO, and H_2O (Chen et al., 2010; Karion et al., 2013; Filges et al., 2015). These observations have proven particularly valuable for quantifying emissions from individual, large emitting point sources (Conley et al., 2017; Mehrotra et al., 2017) as well as constraining emissions of highly heterogeneous processes on 10-100 km scales (Karion et al., 2015; Peischl et al., 2015; Smith et al., 2015; Kort et al., 2016). Continuous, 1 Hz airborne sampling of N_2O with high accuracy and precision has proven more elusive, with limited aircraft

campaigns reporting continuous airborne N_2O (Kort et al., 2011; Wofsy, 2011; Xiang et al., 2013), systems being large and challenging to operate with frequent attention to supplies of cryogens (Santoni et al., 2014), and newer systems showing large cabin pressure dependencies (Pitt et al., 2016).

N_2O is a potent greenhouse gas with natural and anthropogenic sources, and is currently the single most impactful anthropogenic ozone-depleting substance actively emitted to the atmosphere (Ravishankara et al., 2009). Atmospheric emissions of N_2O have been steadily rising over time (Myhre et al., 2013), but attempts to better quantify, understand, and constrain anthropogenic emissions have been hindered by high uncertainties in model estimates and limited observational constraints (Ciais et al., 2013; Davidson and Kanter, 2014). The poor understanding of N_2O emissions processes is attributable to a combination of high spatial and temporal variability (Monni et al., 2007) that is hard to observe and represent, and a lack of direct observational data of emissions sources (Brown et al., 2001). The largest source of anthropogenic N_2O, contributing 66% of global N_2O emissions, is agricultural activity (Davidson and Kanter, 2014). Some of these emissions are a direct product of human activity, such as the fertilizer production process, which has grown to 100 Tg N yr^{-1} since the development of the Haber-Bosch process in 1908 (Erisman et al., 2008). Other anthropogenic emissions, such as from applied fertilizer, are harder to observe and represent as environmental factors including soil moisture, temperature, and crop type all influence emissions (Dalal et al., 2003; Ruser et al., 2006; Griffis et al., 2017).

A diverse range of approaches have been utilized in attempts to measure N_2O emissions (Denmead, 2008; Rapson and Dacres, 2014). Flux chambers can quantify emissions from areas on the order of square meters (Bouwman et al., 2002; Marinho et al., 2004; Turner et al., 2008; Chadwick et al., 2014). Given the heterogeneity in N_2O emission processes, extrapolation of limited flux chambers to accurately represent domains on the orders of 10-100 square km remains challenging (Pennock et al., 2005; Flechard et al., 2007). The eddy covariance approach deploys sensors on towers to estimate fluxes on a 1-10 km^2 scale (Dalal et al., 2003; Pattey et al., 2007), but not beyond that range, thus encountering similar representation challenges as flux chambers. Bottom-up modeling of emissions processes (Del Grosso et al., 2006; Tian et al., 2015) can represent emissions at a range of scales. The models are typically trained and evaluated with data from flux-chambers and then simulate emissions at a continental to global scale. Evaluation of these representations then can happen at the larger scales, where top-down atmospheric inversions (Kort et al., 2008, 2011; Miller et al., 2012; Thompson et al., 2014; Chen et al., 2016; Griffis et al., 2017; Nevison et al., 2018) have challenged modeled and inventoried emissions and often found large discrepancies exceeding 100% (Miller et al., 2012). To better understand these divergences as well as to properly assess the representation of flux-chamber and eddy covariance measurements, we need observational constraints at 10-100 square km spatial scales.

Continuous, 1 Hz airborne measurements can provide information at this critical spatial scale, in addition to providing observational constraints for large point sources (N_2O fertilizer production facilities present a potentially important source of N_2O emissions). To get good, useful data, aircraft studies require instruments that have high precision, a fast response time, and are relatively robust to changes in the environment (Fried et al., 2008). Continuous-wave tunable infrared laser direct absorption spectrometers (CW-TILDAS) can satisfy those requirements and are an appropriate choice for airborne instrumentation (Rannik et al., 2015).

~~Mid-infrared~~ Infrared laser spectrometers have been widely used in airborne studies. They often employ an in-flight calibration to correct for spectral drift that can occur over several hours of measurement (O'Shea et al., 2013; Santoni et al., 2014). Zero air with no gases in the absorption spectrum can also be used to adjust the spectral baseline for more accurate measurements, particularly if the desired gas has a weak absorption feature (Yacovitch et al., 2014; Smith et al., 2015). One recent study to measure N_2O emissions with such an instrument reported their assessment of its performance and found artifacts in the data primarily due to changes in airplane cabin pressure (Pitt et al., 2016), significantly impacting the duty cycle of the analyzer and its utility during vertical profiles. To deploy a CW-TILDAS for N_2O observation as in Pitt et al. (2016), problems can arise if drifts occur on a timescale faster than the conventional calibration period of 0.5-1 hour. Also, at low flow rates (0.1 - 1 slpm), N_2O can take a long time to equilibrate, and this can have a negative impact on the instrument's duty cycle (Santoni et al., 2014). The efficacy of airborne instrumentation for N_2O measurements would benefit from improvements to such limitations.

We present the Frequent Calibration High-performance Airborne Observation System (FCHAOS), utilizing a TILDAS instrument and ~~a novel~~ an updated calibration technique, to make N_2O measurements that can be utilized for calculating facility emissions, mass balance fluxes, and regional inversions. Rather than relying on spectral zeros and infrequent in-flight calibrations to correct for drift on large time-scales, we use short, frequent calibration measurements to resolve both long-term spectral drift and short-term environmental effects. This research was part of the Fertilizer Emissions Airborne Study (FEAST) campaign in spring 2017 targeting N_2O and other greenhouse gas emissions in the southern Mississippi River Valley region of the USA. In this manuscript we discuss the operation and set-up of the instrumentation involved in the airborne flight system. We discuss test flights done to assess the off-the-shelf operation and the associated flaws. We then present our solution to improve instrument performance with short, frequent calibrations and validation by in-flight calibrations and comparison with a flight-proven Picarro cavity ring-down spectrometer.

2 Instrumentation

2.1 CW-TILDAS description

The core of our system is an Aerodyne mini spectrometer. The spectrometer uses a mid-IR, continuous-wave, distributed feedback laser with a frequency of 2227 cm^{-1} (nanoplus, Germany). The laser is mounted on a copper Peltier device which keeps the laser temperature stable at ~17 °C and is regulated by a thermoelectric chiller held at 23 °C (Oasis 3, Solid State Cooling, USA). This laser is optically aligned into a 0.5 L astigmatic mirror multipass absorption Herriott cell (McManus et al., 1995). The refraction pattern in the cell is optimized to produce a total path length of 76 meters before the beam exits the cell and is aligned into a photodetector. The cell itself is sealed and held at ~40 Torr. The space outside of the cell is subject to variations in external pressure. The laser's output frequency can be adjusted by ramping the current, sweeping across a frequency range of approximately 2227.4-2227.9 cm^{-1}. This range contains transition lines for H_2O, CO_2, CO, and N_2O, allowing the photodetector to measure the laser transmission intensity at each of these transitions (Nelson et al., 2002).

The mole fractions of N_2O, CO_2, CO, and H_2O are reported using the TDLWintel software as described in Nelson et al. (2002) and Nelson et al. (2004). The retrieval uses the Beer-Lambert law, where the absorption intensity, path length, and molar

absorptivity enable calculation of gas ~~concentration~~mixing ratio. The absorption spectrum is fit in real-time with a Voigt density profile using the Levenberg-Marquardt algorithm, allowing retrievals at 1 Hz (Nelson et al., 2004). The exact frequencies of the line transitions and absorption cross-sections are obtained from the HITRAN2012 database (Rothman et al., 2013). Pressure and temperature data acquired from sensors in the cell are used to account for broadening effects in the fit. ~~Though initial measurements are made as wet molar fractions, TDLWintel uses a H_2O broadening coefficient to mitigate the effect of H_2O vapor, directly reporting dry molar fractions for N_2O, CO_2, and CO (Lebegue et al., 2016; Pitt et al., 2016).~~

2.2 Set-up and payload

We integrated the FCHAOS system on a single-engine Mooney M20R aircraft from Scientific Aviation. Figure 1 shows the flow diagram for our system. The inlet line to the instrument is ~5 m PVDF Kynar tubing. The inlet line is rear-facing on the right wing to reduce liquid and particle contamination of the line, with the plane exhaust located on the left wing, minimizing exhaust contamination. A membrane disc filter (Pall, USA) is also used to block particulates from entering the cell. Using a mass flow controller (MC-5SLPM-D, Alicat Scientific, USA), we set a flow rate of 1.5 slpm. The MFC is placed downstream of the filter to prevent damage due to rogue particulates. The instrument cell is pressurized on the ground to 40 Torr using a dry scroll pump (IDP-3, Agilent Technologies, USA) and a needle valve (SS-1RS4, Swagelok, USA) directly upstream of the pump for adjusting the target pressure given a defined mass flow rate. The use of mass flow control enables rapid switching between calibration gas and ambient air without inducing pressure fluctuations or ~~pressure~~ ringing in the cell. The mass flow control setup is a closed system (no excess flow), thus ensuring no contamination of other inlets and minimal waste of calibration gas. Pressure-control systems that are optimally tuned may achieve similar performance, but even with an excess flow to reduce pressure pulses, it is difficult to reach similar performance as with mass flow control. Figure 2 illustrates respective performance in-flight of a pressure and mass flow control configuration for our instrument. Two 2 L aluminum carbon-fiber-wrapped compressed air cylinders are securely strapped in the plane. These tanks are outfitted with stainless steel regulators (51-14B-590, Air Liquide, USA) and stored calibration gases. Two three-way solenoid valves (009-0294-900, Parker-Hannifin, USA) control the air flow between the tanks and the inlet line.

The additional payload is set up on the Mooney as described in Conley et al. (2014) and Conley et al. (2017). Temperature and relative humidity are recorded with a humidity probe (HMP60, Vaisala, Finland). A cavity ring-down spectrometer (G2301-f, Picarro, USA) measures CH_4, CO_2, and H_2O as described in Crosson (2008). Ozone is measured with an ozone monitor (Model 202, 2B Technologies, USA). Wind speed and direction are calculated using a differential GPS method as in Conley et al. (2014). The Mooney aircraft is not pressurized, so the instrument experiences pressure variation as the aircraft profiles.

Lag time between when air enters an instrument's inlet line and when it is measured in the cell is determined by breathing close to the inlet tube and recording sharp rises in CO_2 and H_2O ~~concentrations~~mixing ratios. For FEAST lag times were measured at 3 s and 5 s for the FCHAOS and Picarro G2301-f respectively, values confirmed in flight by comparing variability with temperature and RH data from the humidity probe. These lag times are used in post-processing to match avionics and GPS data with the co-located ~~mole fraction concentrations~~ molar ratios from the FCHAOS and G2301-f. Though lag times will

vary with altitude, given the flow-rates, inlet line volumes, and altitude range of the Mooney aircraft it is essentially constant for the data presented in this manuscript.

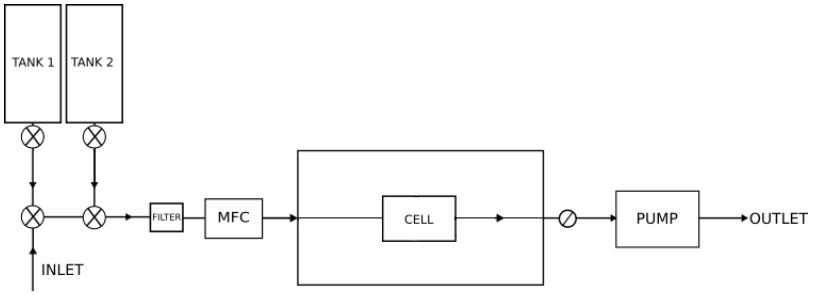

Figure 1. Schematic of FCHAOS, where air flows from the inlet line through the solenoid valves, past the filter to the mass flow controller (MFC), through the instrument cell, a needle valve, and finally the vacuum pump. When calibrating the solenoid valves are actuated to direct flow from each individual calibration tank into the cell directly.

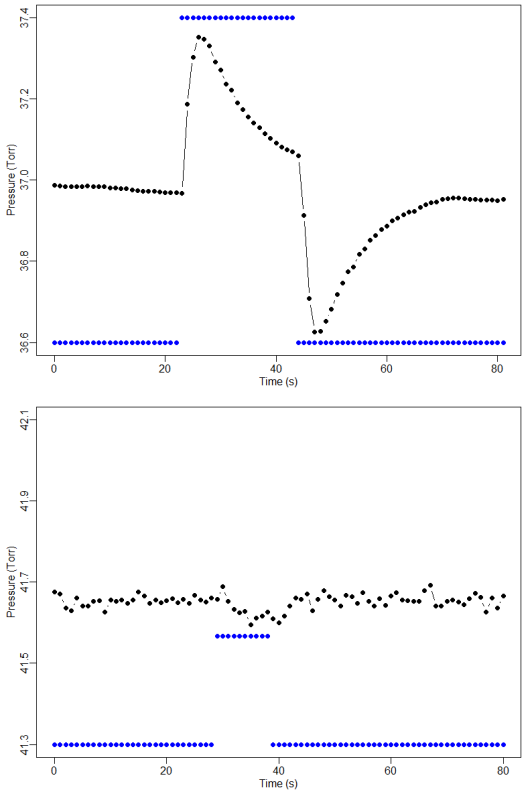

Figure 2. Cell pressure (black) in response to actuating a solenoid and sampling a standard cylinder (blue indicates solenoid position). The pressure control setup (top panel), including excess flow, exhibits significant pressure perturbations and residual transients that persist longer than desired calibration time. The mass flow control setup (bottom panel) shows pressure perturbations of shorter duration and on the order of 0.04 Torr, 20 times smaller than with pressure control.

2.3 Calibration

We performed pre-flight calibrations on the ground for both the FCHAOS and Picarro G2301-f using two air cylinders calibrated to a NOAA WMO greenhouse gas scale (X2007, X2004A, X2014A, X2006A for CO_2, CH_4, CO, and N_2O respectively) (WMO, 2015). Both cylinders had ~~concentrations~~ mixing ratios of CO_2 (Zhao et al., 1997; Zhao and Tans, 2006; Tans et al., 2017), CH_4 (Dlugokencky et al., 2005), CO (Novelli et al., 2003), and N_2O (Hall et al., 2007) near ambient atmospheric levels, with one as a high-span standard and the other as a low-span.

We sequentially sampled these cylinders for multiple cycles, and compared the measured ~~concentration~~ mixing ratios for each gas to the reported value on the WMO scale. We consider known values X_{true} against the measured values $X_{measured}$, and a linear fit provides the slope m and intercept b such that $X_{true} = m*X_{measured} + b$.

We filled the two in-flight calibration tanks used with the FCHAOS for FEAST with a separate custom mixture that contained atmospheric levels of N_2O, CO_2, and CO. We calibrated the ~~concentrations~~ mixing ratios using the WMO standard cylinders

by sampling the target cylinders in between the WMO standards. During flights, we used one tank as a single-point calibration gas, while the other was used as a check gas to assess the instrument's traceability. We elaborate on these processes in Sect. 3.2 and 4.1.

We assessed the stability in ~~linearity~~ slope of the instrument by performing calibrations separated by months before and after the FEAST campaign. Over the course of four months, the slopes for N_2O, CO_2, and CO changed by 0.4%, 0.01%, and 0.5%. The impact of any variation in ~~linearity~~ slope depends on the difference between ambient levels and calibration gas values. For the operation of FCHAOS, we use calibration gas with ~~concentrations~~ mixing ratios near ambient levels. Typical atmospheric ambient levels of N_2O are ~335 ppb, so with a calibration gas at ~330 ppb, the long-term variation due to linearity is 0.4% of 5 ppb, or 0.02 ppb, an uncertainty that is within our 1 Hz precision as reported in Sect. 4.1. For CO_2 and CO, which have ambient atmospheric levels of ~400 ppm and ~155 ppb, we use calibration gases with ~390 ppm and ~150 ppb, and the impacts due to variation in ~~linearity~~ slope are 0.01 ppm and 0.025 ppb, respectively. If zero air were used instead, the impact on N_2O would be on the order of 0.4% of 335 ppb, or 1.3 ppb, an order of magnitude larger, with similar impacts for CO_2 and CO. By using calibration gases close to ambient levels we eliminate our sensitivity to drift in ~~this~~ the instrument's ~~linearity~~ slope and thus can ~~use one~~ a single gas target for in-flight calibration to correct only for intercept variability.

2.4 Water vapor

Spectroscopic measurements of atmospheric species are sensitive to dilution and broadening effects due to water vapor (Chen et al., 2010, 2013; Rella et al., 2013). TDLWintel, in its retrieval algorithm, corrects for water dilution and uses H_2O broadening coefficients to mitigate the effect of water vapor on the spectral lines, directly reporting dry molar fractions for N_2O, CO_2, and CO (Lebegue et al., 2016; Pitt et al., 2016). This coefficient is the ratio of spectral line broadening due to water pressure compared to air pressure broadening. To determine the coefficients, we conducted a test where dry tank air was sampled with varying amounts of water vapor. We used a similar approach as in Lebegue et al. (2016). We used a moist filter along with variable flow through parallel dry tubing, enabling some control of the water vapor content by modulating the relative flows over the moist filter compared to the dry tubing. We sampled at varying humidity starting at ~1.6% H_2O and decreasing to near 0, spanning a typical range of atmospheric water vapor. Using spectral playback in TDLWintel, we were able to re-analyze the spectra with various broadening coefficients until we found the optimum values as in Pitt et al. (2016). Figure 3 shows the measurement data from the test using our optimized broadening coefficients of 1.33, 1.93, and 1 for N_2O, CO_2, and CO, respectively. The dry value is determined from prolonged sampling of dry air only from the standard tank. The deviation from this is shown as a function of water vapor. The gray line shows a moving average with a 10 s window. The RMS difference in N_2O, CO_2, and CO was 0.023 ppb, 0.076 ppm, and 0.75 ppb, respectively. These are used as the uncertainty in water vapor correction, as in Pitt et al. (2016). For CO, a coefficient of 1 corresponds to purely a dilution correction. Larger values of the coefficient do not improve the dependency. As highlighted by Pitt et al. (2016), water broadening coefficients must be determined by users for their own instrument as these can vary for each analyzer and can introduce substantial errors in correcting to dry air mole fraction.

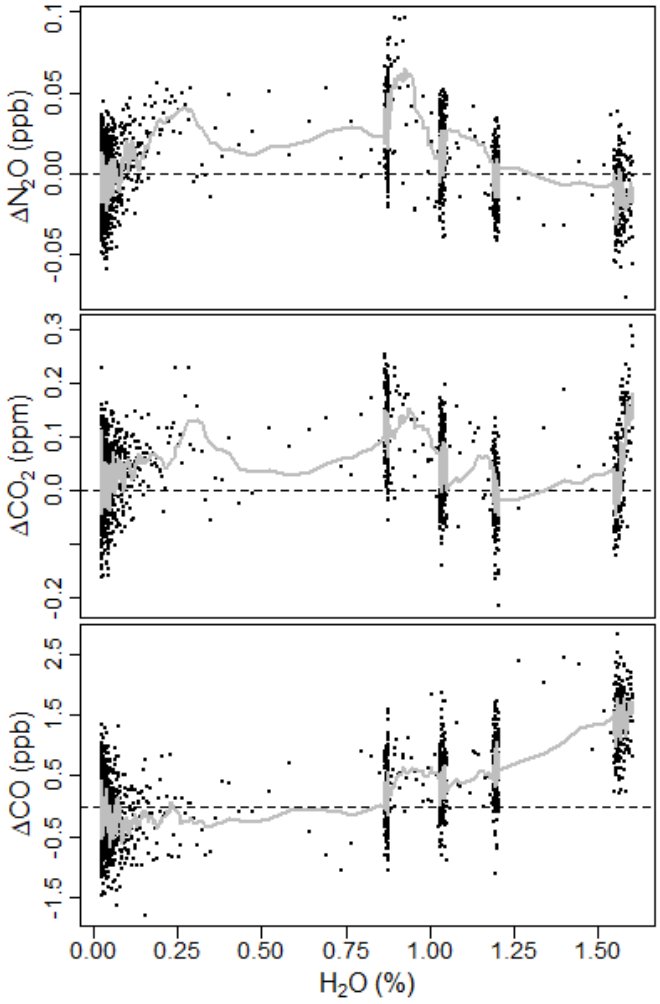

Figure 3. Residual uncertainty in Water vapor correction for N_2O, CO_2, and CO with broadening coefficients of 1.33, 1.93, and 1, respectively. Black dots are the deviation from the dry value, with a moving average (10 s) depicted in gray.

3 In-flight operation

3.1 Null Test

For an instrument to be well-suited for airborne observation, resistance to environmental effects is paramount. A "null test," where an instrument samples air with known ~~concentrations~~ mixing ratios in flight while subject to variation in cabin pressure, air temperature, etc., can be useful in evaluating its robustness as shown in Chen et al. (2010) and Karion et al. (2013). We conducted two null tests using the FCHAOS, once during a test flight in Colorado, once during a research flight in our target region in the lower Mississippi River basin. Figure 4 shows N_2O, CO_2, and CO ~~concentrations~~ mixing ratios observed by the

FCHAOS while sampling tank air during a vertical profile descent. As the altitude decreases, there is a clear dependence due to the cabin pressure changing similar to what was reported in Pitt et al. (2016). As mentioned in Sect. 2, though the cell is pressurized, the rest of the instrument is not, and since the aircraft cabin is not pressurized, our system thus experiences any change in ambient pressure. Correcting or mitigating this cabin pressure artifact is necessary for ~~the~~ FCHAOS to be capable of accurate airborne in-situ sampling.

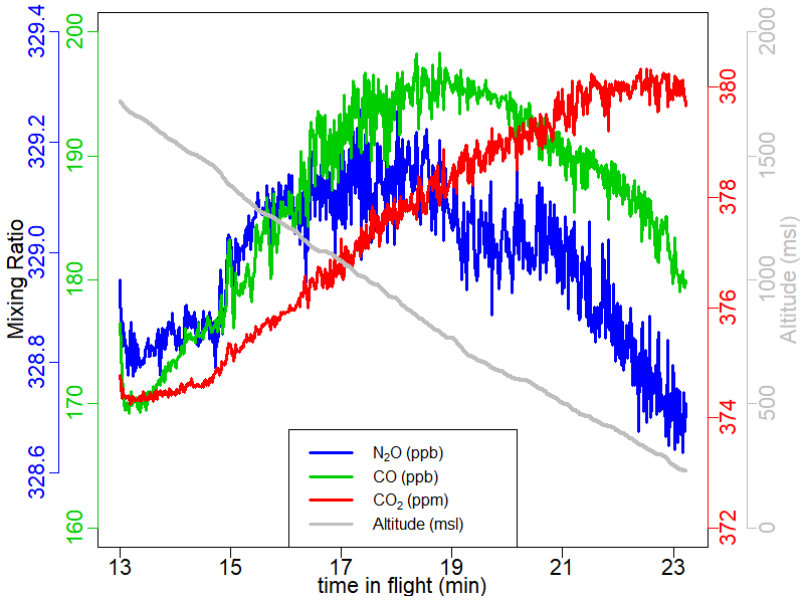

Figure 4. A null test demonstrates artifacts when operating the instrument in an off-the-shelf manner. Drift occurs in N_2O, CO_2, and CO due to changes in cabin pressure that occur with changing aircraft altitude.~~Dry tank air is used for the null test so H_2O is not evaluated.~~

3.2 Frequent calibration correction

The cause of the cabin pressure dependence is not immediately evident. One possible explanation could be an optical fringe pattern in the absorption spectrum that moves with changing cabin pressure. Acceleration during altitude change could also create g-force or electrical (via engine surges) changes that propagate through the instrument system. Without needing to pinpoint the cause, we know the time period of the artifact presents on the order of many minutes, with a typical aircraft climb rate of 500 ft/min. Thus a correction that occurs on a shorter time spacing could remedy the drift. To account for both spectral drift in the instrument that occurs on the order of hours and cabin pressure-related artifacts that emerge on the order of minutes, we developed an empirical correction procedure using frequent measurements of a calibration gas.

The procedure is as follows. Every 2 min, we ~~activate~~ actuate the solenoid valve to sample tank air for 10 s. We determined the calibration frequency of 2 min through a sensitivity test using null test data. By adjusting the calibration frequency and measuring the precision, we found similar 1σ uncertainties at 1 min and 2 min frequencies, but an increase in uncertainty at 4 min and beyond, making 2 min good for reducing gas consumption while maintaining high precision. We allow 5 s of flush

time, leaving 5 s of measurement time. We determined the flush time duration of 5 s by sampling tank air in a lab setting at the ~~appropriate~~ same flow-rate and cell pressure as in-flight operation and measuring equilibration time. We calculate the average measured mole fraction of N_2O, CO_2, and CO in these 5 s~~(we omitted H_2O from this correction as the cabin pressure dependence does not seem to affect H_2O, more in Sect. 4).~~. Figure 5 demonstrates a typical in-flight calibration.

For each species we then interpolated in time using a Forsythe, Malcom, and Moler cubic spline between each measured calibration gas value and subtracted the known "true" value from this interpolation, giving us correction as a function of time. We then subtract this calibration curve from the raw data. Figure 6 shows both raw CO_2 data and the correction we derive using the frequent calibration method from one of our flights. As mentioned above, the gas was on for 10 s, along with 5 s of post-calibration time removed to account for equilibration back to ambient sampling, resulting in a loss of 15 s of atmospheric observations every 120 s for an 87.5% duty cycle. As mentioned in Sect. 2.3, the calibration cylinder ~~concentrations~~ mixing ratios are near atmospheric values. As seen in Santoni et al. (2014), N_2O can take a long time to equilibrate between measurement sources due to its propensity to stick to tubing. Thus, choosing calibration values close to ambient is critical for maintaining short flush times. This also holds for CO_2, though less so for CO. Artifacts that occur on shorter time-frames, such as those induced by a short-duration turbulence event, will not be corrected with this method.

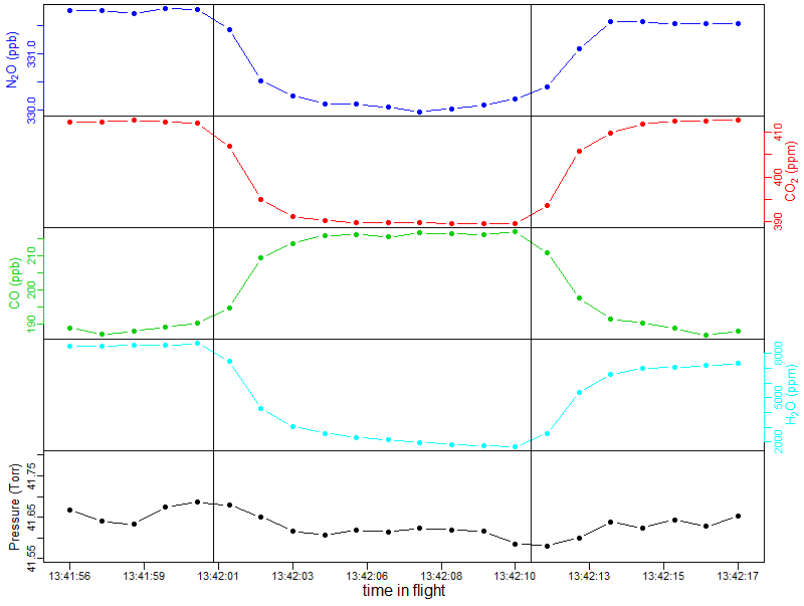

Figure 5. Example of in-flight calibration, showing time series of N_2O, CO_2, CO, H_2O, and cell pressure. Vertical lines indicate when the solenoid valve was actuated or closed. The first 5 seconds of each calibration are treated as equilibration time, and the last 5 seconds are used to find a mean calibration value.

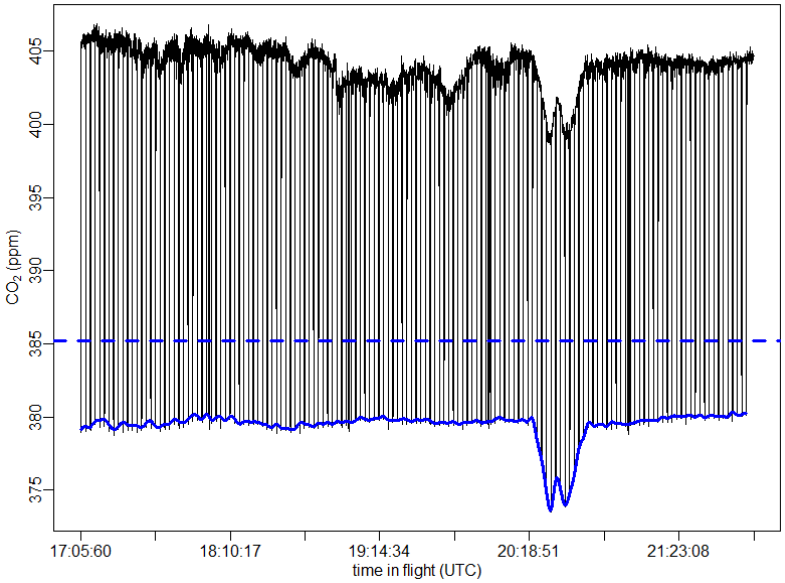

Figure 6. Raw CO_2 (black) measured by the FCHAOS for an entire flight, with frequent low dips due to calibrations. The blue dashed line indicates the "true" value of the calibration gas, the blue solid line shows the calibration curve obtained by interpolating between each calibration instance. The difference between the dashed and solid blue lines is used to correct for drift.

4 Calibration results and comparison with Picarro G2301-f

Figure 7 shows measurements from two null tests, one on April 26, 2017 in Colorado and one on May 2, 2017 in the Mississippi River Valley, the same null test as from Fig. 4. For each null test, the figure shows both the raw N_2O, CO, and CO_2 measurements and the corrected data following our calibration, along with the aircraft altitude. Our calibration method accounts for the clear cabin pressure/altitude dependence. During a null test ~~the~~ FCHAOS samples tank air uninterrupted, rather than making a calibration measurement every 2 min as in the frequent calibration procedure described in Sect. 3.2. Thus, we average 5 s of data from every 120 s to simulate the normal operation mode. Even after correction there is some residual coherent variability evident at the 15 min mark of the null test shown in the bottom 2 rows of Fig. 7, but this potential feature remains still within our ~~instrument~~ 1 Hz precision.

Given the repeatable, smooth nature of the cabin pressure artifact, it ~~is~~ would seem possible to use just the cabin pressure data to empirically correct for the artifact, without running frequent calibrations. This method ~~does~~ would not account for long-term spectral drift however or traceability, ~~compromising accuracy. Additionally, for flights conducted in regions at a different elevation than the one in FEAST, the pressure-correction-only method would require a new vertical profile null test, which can impact gas consumption and flight hour usage.~~ and relies on the assumption that the cabin pressure artifact will be stable and repeatable. These weaknesses compromise such an approach.

Figure 8 compares the raw CO_2 data from the Picarro G2301-f and FCHAOS during a research flight along with altitude, and a second comparison once the FCHAOS data is corrected. The difference between the two instruments is shown in the top 2 panels. The most significant discrepancies occur during the vertical profile section of the flight. Following calibration, the deviation during profiling is eliminated, and the 1σ uncertainty in the difference is reduced from 1.15 ppm to 0.28 ppm.

For the FEAST campaign, in post-processing it became evident that a persistent offset of ~~0.60~~ 0.51 ppm existed for CO_2 between the Picarro and FCHAOS. ~~On multiple subsequent deployments of these analyzers we have not found such offset~~For the CO_2 comparisons in this manuscript, we have corrected for this bias. We believe the origin of this offset to be related to regulator contamination of a calibration gas cylinder and/or tubing used in conjunction with the regulator. ~~For the CO_2 comparisons in this manuscript, we have corrected for this bias~~With subsequent investigation it has been difficult to identify the exact cause. We do note that in comparing the Picarro and FCHAOS instruments, they both are calibrated with dry tank air, whereas the in-flight comparison is while measuring wet ambient air. Any residual water vapor sensitivity not corrected for either analyzer can manifest as an apparent bias, and this further emphasizes the need to validate water vapor corrections, as pointed out by Pitt et al. (2016), and further outlined for FCHAOS above in the discussion of the water vapor correction.

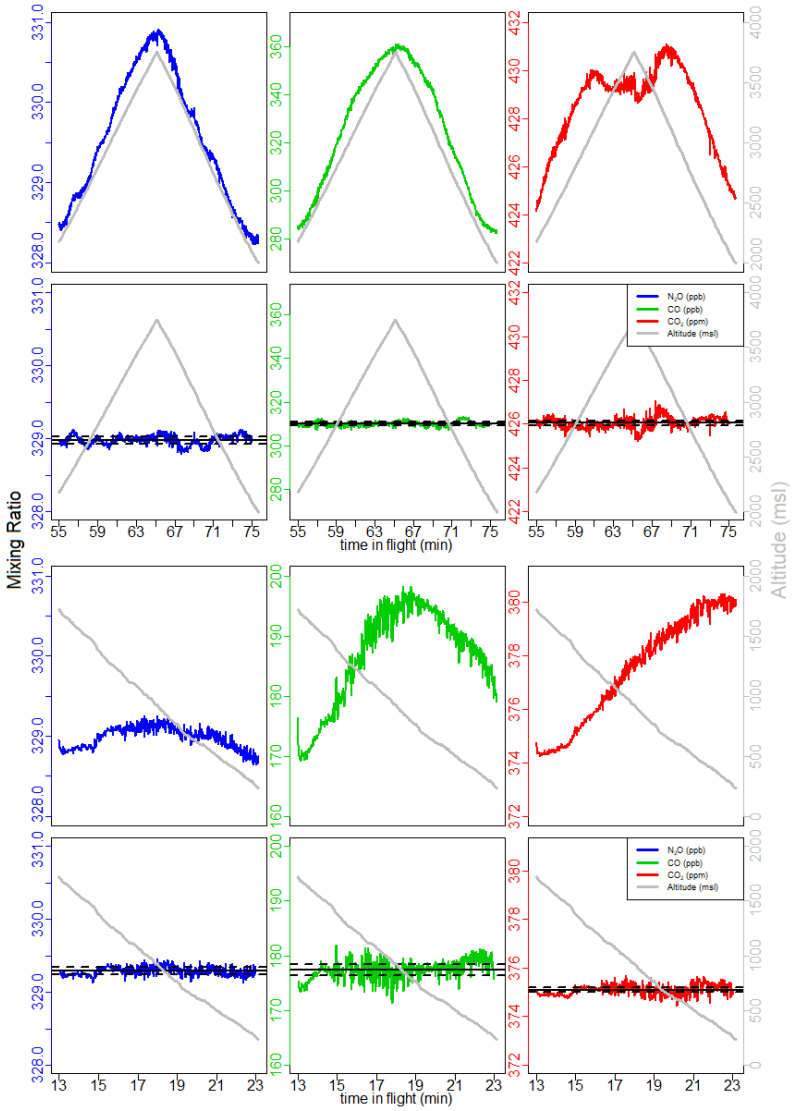

Figure 7. Top two rows show FCHAOS data from a null test on April 26, 2017, bottom two rows shows data from a null test on May 2, 2017, the same seen in Fig. 4. Rows 1 and 3 show N_2O, CO, and CO_2 during the null test before any calibration, rows 2 and 4 show the gas data following the frequent calibration correction. The procedure removes cabin pressure dependence and calibrates for linear drift. Black horizontal lines show mean and 1σ uncertainty.

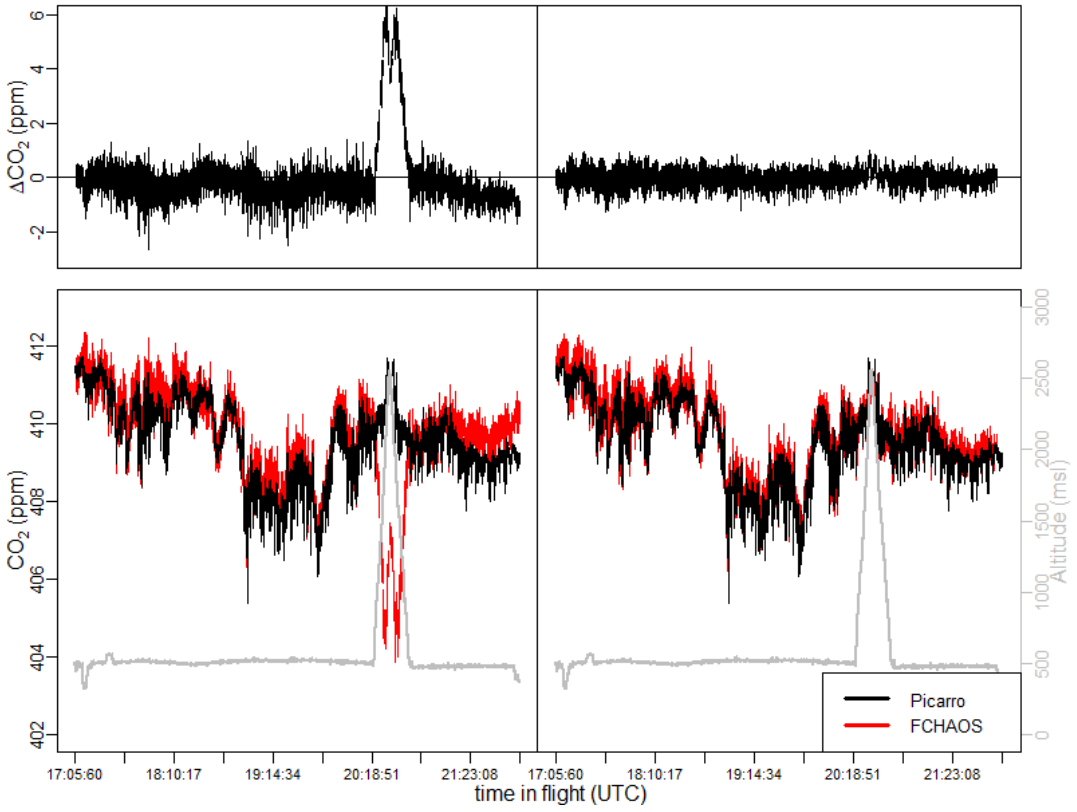

Figure 8. Bottom panels show Picarro G2301-f and uncalibrated FCHAOS CO_2 time series on left, Picarro G2301-f and calibrated FCHAOS CO_2 on right. Top panels show difference between the two instruments with and without FCHAOS calibration. The calibration procedure corrects for any artifacts in the FCHAOS data correlated with aircraft altitude.

The raw H_2O measurements exhibit good agreement between FCHAOS and the Picarro G2301-f. The H_2O data was not calibrated or adjusted in any way, as there appeared to be ~~minimal, if any,~~ small impact from cabin pressure variance and it is not well characterized. Figure 9 shows a histogram of the differences in FCHAOS and Picarro G2301-f ~~and FCHAOS~~ H_2O and CO_2 (following calibration) for ~~over 40~~ ~40 hours of research flight time. Figure 10 shows the differences as a function of time for all flight data. For H_2O, we find a mean difference between the two instruments of ~~170~~ 180 ppm, a median of 180 ppm, and 1σ of 340 ppm, shown in the figures as solid and dashed lines. In-flight 1σ precision for H_2O from the Picarro G2301-f has been reported as 100 ppm (Crosson, 2008), while the in-flight 1σ precision for the FCHAOS was found to be 10 ppm. ~~If a moving fringe is indeed the culprit for the cabin pressure sensitivity, it is possible that it does not manifest for~~

Why does water vapor not exhibit the same sensitivities as the other gases? To assess the sensitivity for water vapor to cabin pressure is more challenging given the long equilibration time. In Fig. 11 we show H_2O ~~, which has the lowest transition frequency and highest laser intensity, likely resulting in the best signal-to-noise compared to N_2O, CO_2, and CO. The width of the fringe may be narrower than the absorption band, and does not impact~~ during the null test. On the null test where water vapor has previously equilibrated, some altitude-dependent sensitivity is apparent (~60 ppm). Our calibration approach

cannot well address this potential residual sensitivity given the long equilibration time required for H_2O~~as much as it does the other gases.~~. Does this potential artifact matter? In comparison with the Picarro analyzer (Fig. 11) we see no evident residual sensitivity to altitude. Given relative uncertainties, we cannot eliminate the presence of a vertical sensitivity of 10s ppm for water vapor.

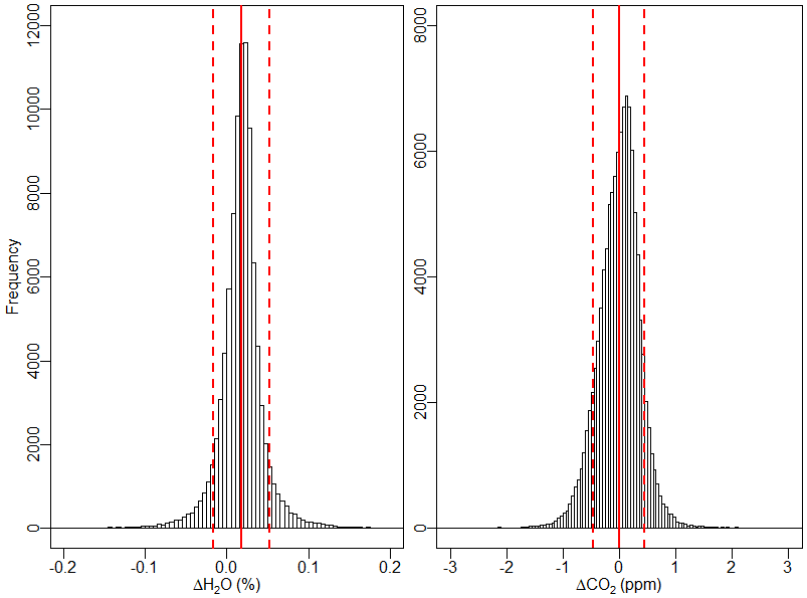

Figure 9. Histogram of difference between H_2O and CO_2 ~~concentrations~~ mixing ratios from FCHAOS and the Picarro G2301-f~~and FCHAOS~~. FCHAOS CO_2 has been calibrated, while H_2O has not. For H_2O, mean of ~~0.017~~0.018% or ~~170~~ 180 ppm, median of 0.018% or 180 ppm, 1σ of 0.034% or 340 ppm, where Picarro G2301-f precision is 100 ppm. For CO_2, mean of 0 ppm, median of ~~0.01~~ 0.024 ppm, 1σ of ~~0.44~~ 0.45 ppm.

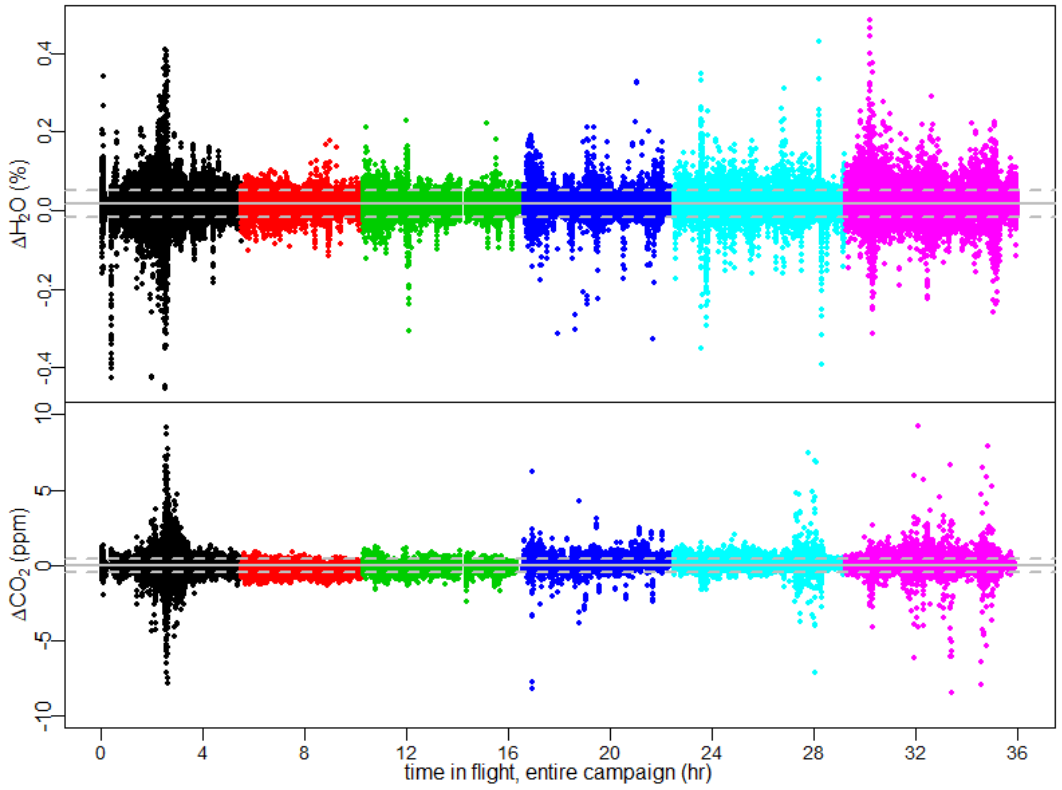

Figure 10. Difference as function of flight time ~~in~~ for FCHAOS and Picarro G2301-f ~~and FCHAOS~~ H_2O and CO_2 for all research flights. Colors separate flight days, ~~grey~~ gray lines indicate mean and 1σ uncertainty. Largest deviations occur when sampling in the immediate near-field of large point sources where some mismatched lag times contribute to deviations.

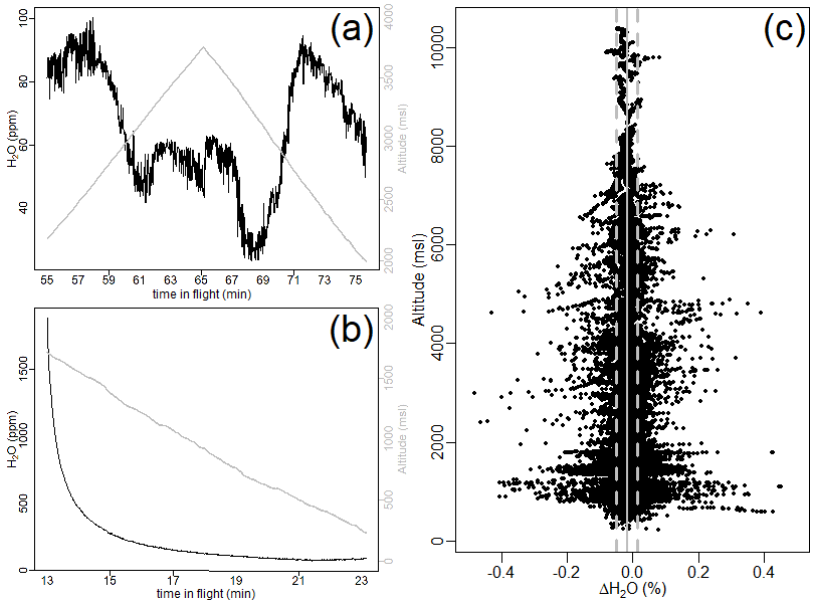

Figure 11. Panels (a) and (b) show H_2O during null tests from Fig. 7. In panel (b) H_2O hasn't fully equilibrated. In panel (a), H_2O previously equilibrated and there does appear to be a dependence on altitude on the order of 60 ppm. As seen in panel (c), the difference in H_2O between the Picarro and FCHAOS over the entire campaign does not exhibit an altitude dependence, so while there may be some altitude sensitivity, the effect is relatively small compared to typical atmospheric concentrations of H_2O and our overall water vapor uncertainty.

4.1 Precision and Accuracy

To assess the FCHAOS precision, we consider flight data during a null test when the altitude did not significantly change. We find 1 s precisions of $\pm$0.05 ppb, $\pm$0.10 ppm, $\pm$1.00 ppb, and $\pm$10 ppm for N_2O, CO_2, CO, and H_2O respectively. This is about a factor of 2 greater than the performance on the ground in a lab setting, with 1σ precisions of 0.02 ppb, 0.05 ppm, 0.50 ppb, and 7 ppm. Considering an Allan variance analysis of both the in-flight null test and in-lab study, the same result holds, in that the Allan variance in the air closely matches the ground, with performance degraded by a factor of 2.

In addition to the frequent calibrations every two minutes, a second cylinder is sampled every hour for 25 s as a "check gas" to test the traceability of the in-flight system. The last 5 s of each check gas period is used to calculate a mean value for each species. Figure 12 shows each instance of N_2O, CO_2, and CO check gas sampling, along with histograms for the difference from the known value. The time series show the last 5 s of each check gas period, along with a horizontal line indicating the known value of the air tank calibrated with the WMO standards as in Sect. 2.3. Note that the "check gas" and "calibration gas" cylinders were switched halfway through the campaign due to gas consumption, as reflected by the horizontal line. Looking at the difference of each check gas period from the known value, we find median offsets of ~~0.17 ppb, 0.08~~ 0.06 ppb, 0.06 ppm, and ~~0.29~~ 0.03 ppb for N_2O, CO_2, and CO respectively, representative of possible bias between the flight system and the WMO scale. The 1σ values for the check gas points are ~~0.13 ppb, 0.34~~ 0.10 ppb, 0.30 ppm, and ~~2.33~~ 1.62 ppb for N_2O, CO_2, and CO,

representative of traceability of individual 1 s observations to the WMO scale. Table 1 summarizes the precision and accuracy for the four gases, though we were unable to measure H_2O traceability because we calibrated with dry tank air. We do report water vapor (and carbon dioxide) performance in comparison with the Picarro. Total instrument 1 s uncertainty is derived from summing in quadrature the 1σ accuracy to WMO, water vapor correction, and standard tank calibration uncertainty.

Table 1. Precision and accuracy for N_2O, CO_2, CO, and H_2O.

	N_2O (ppb)	CO_2 (ppm)	CO (ppb)	H_2O (ppm)
1σ Precision	0.05	0.10	1.00	10
Accuracy (median offset)	~~0.17~~ 0.06	~~0.08~~ 0.06	~~0.29~~ 0.03	NA
1σ comparison with Picarro	NA	0.45	NA	340
Accuracy (1σ check gas)	~~0.14~~ 0.10	~~0.34~~ 0.30	~~2.33~~ 1.62	NA
Water vapor correction	0.023	0.076	0.75	NA
WMO standard calibration	0.26	0.11	0.71	NA
Total 1σ uncertainty	0.28	0.33	1.92	NA

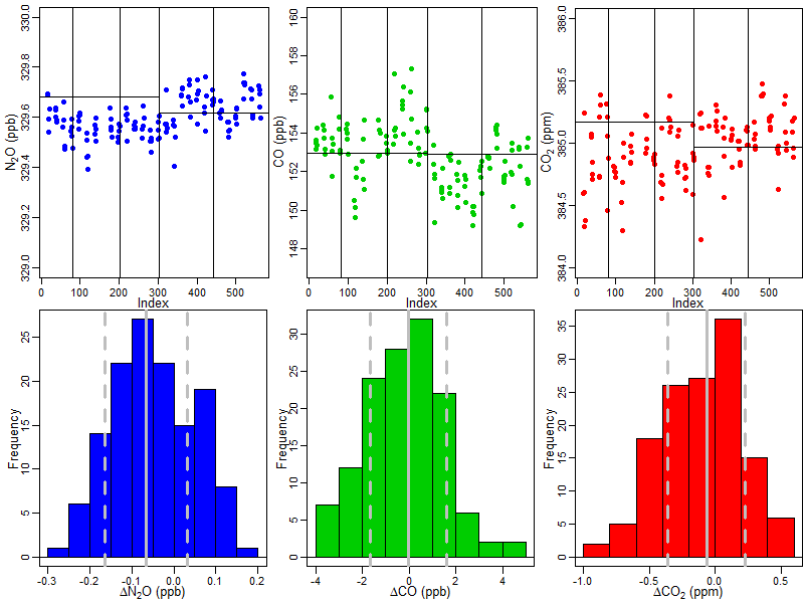

Figure 12. Top row: the last 5 s of each check gas period, black horizontal line indicating the value of the sampled gas traced to the WMO scale. Vertical lines separate the individual research flights. Bottom row: histograms of difference between known check gas value and last 5 s of measured check gas value, with solid ~~grey~~ gray lines indicating median and dashed lines showing 1σ uncertainty.

5 Applications

Continuous airborne N_2O observations can be useful for quantifying fluxes and estimating emissions on a facility-to-regional scale. Mass balances techniques, which have been utilized to estimate emissions of other atmospheric gases as in Karion et al. (2013), Smith et al. (2015), Peischl et al. (2015), and Kort et al. (2016), could similarly be applied for N_2O. Figure 13 shows the path flown during a research flight on May 6, 2017, with measured N_2O mole fraction in color, white arrows indicating wind direction and speed, and blue and black arrows showing the direction of the flight route and the upwind and downwind transects. The downwind transect was flown at a mean altitude of 1515 msl, 1σ of 14 m, and the upwind transect at a mean altitude of 1501 msl, 1σ of 14m. The bottom right panel of the figure shows N_2O from this flight as a function of latitude with the upwind and downwind transects in blue and black, while the top right panel shows the difference in N_2O between the downwind and upwind at each latitude. There is a distinct enhancement in the downwind transect relative to the upwind transect in the lower latitudes, from about 31.5° N to 32° N. This enhancement disappears at higher latitudes and the N_2O measurement tracks well between upwind and downwind transects, even with a substantial latitudinal gradient. This flight illustrates the ability of this instrument to accurately measure small variations and link to local emissions (to the south) or larger scale gradients (to the north). Future analyses of this data can involve mass balance flux quantification and/or regional model comparisons, both to quantify emissions and link to driving factors such as soil moisture or crop type.

As a fast-response sensor, FCHAOS can also be used for point source quantifications, as first explained in Conley et al. (2017) and further analyzed in Mehrotra et al. (2017) and Vaughn et al. (2017). During FEAST, we circled several fertilizer plants with significant N_2O emissions, and future analyses can leverage these observations to better quantify emissions from the large point sources.

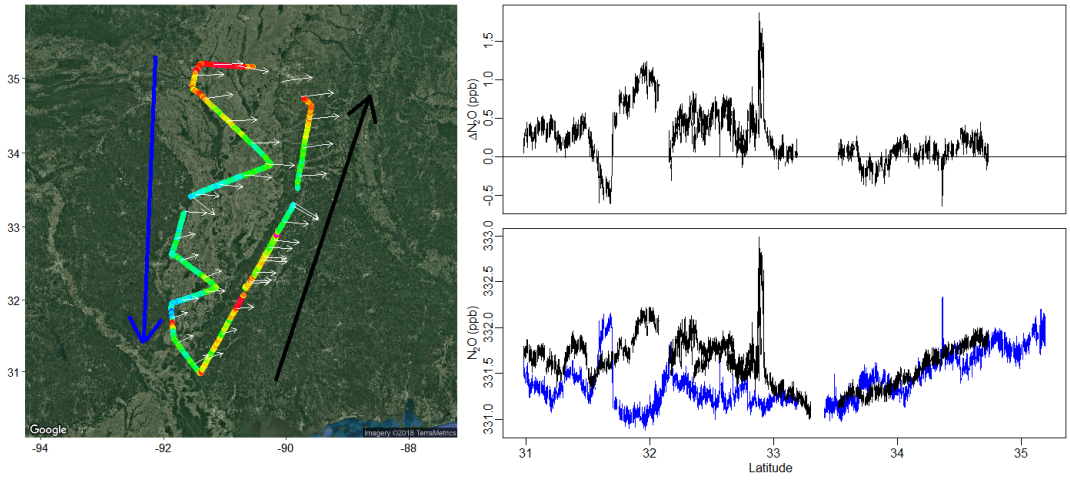

Figure 13. Left panel: flight path with N_2O signal and wind direction (white arrows). Blue and black arrows show the direction of the planes route and indicate upwind and downwind transects. Bottom right panel: N_2O signal as a function of latitude with upwind and downwind transects colored by blue and black, respectively. Top right panel: Difference in N_2O between downwind and upwind transects as a function of latitude.

6 Conclusions

We present a continuous-wave, mid-IR laser spectrometer system that can measure continuous 1 Hz airborne mole fractions of N_2O, CO_2, CO, and H_2O. The commercial analyzer, when operated off-the-shelf, exhibits a dependence of N_2O, CO_2, and CO on cabin pressure. We correct for this artifact by employing ~~a new~~ an updated calibration procedure with mass flow control at a high flow rate enabling high-frequency, short-duration calibrations. While modern systems conventionally use pressure control and infrequent, long-duration zeros, our method expands on these previous approaches and opens up uses for the instrument in ways that have not yet been realized. We solve the inability of other systems to operate with large changes in cabin pressure by mitigating the cabin pressure effect while maintaining a ~90% duty cycle. In-flight 1σ precisions are estimated to be $\pm$0.05 ppb, $\pm$0.10 ppm, $\pm$1.00 ppb, and $\pm$10 ppm for N_2O, CO_2, CO, and H_2O, with ~~traceability to WMO observations estimated at 0.14 ppb, 0.34~~ total uncertainty in traceability estimated at 0.28 ppb, 0.33 ppm, and ~~2.33~~ 1.92 ppb for N_2O, CO_2, and CO. We then validate our method by comparing FCHAOS data to CO_2 and H_2O measurements from a flight-proven cavity ring-down spectrometer, seeing excellent agreement. This flight-proven system can provide key insights into N_2O emissions processes by providing observational support for facility-quantification, for mass-balance flux estimates, and for inverse modeling. As presented, this system can be utilized for precise, accurate, continuous 1 Hz airborne observations of N_2O, CO_2, CO, and H_2O.

Data availability. Kort E.A., Gvakharia A., Smith M.L., Conley S. Airborne Data from the Fertilizer Emissions Airborne Study (FEAST). Nitrous Oxide, Carbon Dioxide, Carbon Monoxide, Methane, Ozone, Water Vapor, and meteorological variables over the Mississippi River Valley [Data set]. University of Michigan Deep Blue Data Repository. https://doi.org/10.7302/Z2XK8CRG

Competing interests. The authors declare they have no competing interests.

Acknowledgements. We thank Scientific Aviation pilots for their efforts in helping collect this data and Aerodyne Research Inc. for useful discussions. This material is based partly upon work supported by the National Science Foundation under Grant No. 1650682.

References

Bouwman, A. F., Boumans, L. J. M., and Batjes, N. H.: Emissions of N2O and NO from fertilized fields: Summary of available measurement data, Global Biogeochemical Cycles, 16, 6–1–6–13, https://doi.org/10.1029/2001GB001811, https://agupubs.onlinelibrary.wiley.com/doi/abs/10.1029/2001GB001811, 2002.

Brown, L., Armstrong Brown, S., Jarvis, S. C., Syed, B., Goulding, K. W. T., Phillips, V. R., Sneath, R. W., and Pain, B. F.: An inventory of nitrous oxide emissions from agriculture in the UK using the IPCC methodology: emission estimate, uncertainty and sensitivity analysis, Atmospheric Environment, 35, 1439–1449, https://doi.org/10.1016/S1352-2310(00)00361-7, 2001.

Chadwick, D., Cardenas, L., Misselbrook, T., Smith, K., Rees, R., Watson, C., McGeough, K., Williams, J., Cloy, J., Thorman, R., et al.: Optimizing chamber methods for measuring nitrous oxide emissions from plot-based agricultural experiments, European Journal of Soil Science, 65, 295–307, 2014.

Chen, H., Winderlich, J., Gerbig, C., Hoefer, A., Rella, C. W., Crosson, E. R., Van Pelt, A. D., Steinbach, J., Kolle, O., Beck, V., Daube, B. C., Gottlieb, E. W., Chow, V. Y., Santoni, G. W., and Wofsy, S. C.: High-accuracy continuous airborne measurements of greenhouse gases (CO_2 and CH_4) using the cavity ring-down spectroscopy (CRDS) technique, Atmospheric Measurement Techniques, 3, 375–386, https://doi.org/10.5194/amt-3-375-2010, https://www.atmos-meas-tech.net/3/375/2010/, 2010.

Chen, H., Karion, A., Rella, C. W., Winderlich, J., Gerbig, C., Filges, A., Newberger, T., Sweeney, C., and Tans, P. P.: Accurate measurements of carbon monoxide in humid air using the cavity ring-down spectroscopy (CRDS) technique, Atmospheric Measurement Techniques, 6, 1031–1040, https://doi.org/10.5194/amt-6-1031-2013, https://www.atmos-meas-tech.net/6/1031/2013/, 2013.

Chen, Z., Griffis, T. J., Millet, D. B., Wood, J. D., Lee, X., Baker, J. M., Xiao, K., Turner, P. A., Chen, M., Zobitz, J., and Wells, K. C.: Partitioning N2O emissions within the U.S. Corn Belt using an inverse modeling approach, Global Biogeochemical Cycles, 30, 1192–1205, https://doi.org/10.1002/2015GB005313, http://dx.doi.org/10.1002/2015GB005313, 2015GB005313, 2016.

Ciais, P., Chris, S., Govindasamy, B., Bopp, L., Brovkin, V., Canadell, J., Chhabra, A., Defries, R., Galloway, J., and Heimann, M.: Carbon and other biogeochemical cycles, pp. 465–570, Cambridge University Press, 2013.

Conley, S., Faloona, I., Mehrotra, S., Suard, M., Lenschow, D. H., Sweeney, C., Herndon, S., Schwietzke, S., Pétron, G., Pifer, J., Kort, E. A., and Schnell, R.: Application of Gauss's theorem to quantify localized surface emissions from airborne measurements of wind and trace gases, Atmospheric Measurement Techniques, 10, 3345–3358, https://doi.org/10.5194/amt-10-3345-2017, https://www.atmos-meas-tech.net/10/3345/2017/, 2017.

Conley, S. A., Faloona, I. C., Lenschow, D. H., Karion, A., and Sweeney, C.: A Low-Cost System for Measuring Horizontal Winds from Single-Engine Aircraft, Journal of Atmospheric and Oceanic Technology, 31, 1312–1320, https://doi.org/10.1175/JTECH-D-13-00143.1, https://doi.org/10.1175/JTECH-D-13-00143.1, 2014.

Crosson, E.: A cavity ring-down analyzer for measuring atmospheric levels of methane, carbon dioxide, and water vapor, Applied Physics B, 92, 403–408, https://doi.org/10.1007/s00340-008-3135-y, https://doi.org/10.1007/s00340-008-3135-y, 2008.

Dalal, R. C., Wang, W., Robertson, G. P., and Parton, W. J.: Nitrous oxide emission from Australian agricultural lands and mitigation options: a review, Australian Journal of Soil Research, 41, 165, https://doi.org/10.1071/sr02064, https://doi.org/10.1071/sr02064, 2003.

Davidson, E. A. and Kanter, D.: Inventories and scenarios of nitrous oxide emissions, Environmental Research Letters, 9, 105 012, http://stacks.iop.org/1748-9326/9/i=10/a=105012, 2014.

Del Grosso, S., J Parton, W., Mosier, A., K Walsh, M., S Ojima, D., and E Thornton, P.: DAYCENT National-Scale Simulations of Nitrous Oxide Emissions from Cropped Soils in the United States, Journal of Environmental Quality, 35, 1451–60, 2006.

Denmead, O.: Approaches to measuring fluxes of methane and nitrous oxide between landscapes and the atmosphere, vol. 309, 2008.

Dlugokencky, E. J., Myers, R. C., Lang, P. M., Masarie, K. A., Crotwell, A. M., Thoning, K. W., Hall, B. D., Elkins, J. W., and Steele, L. P.: Conversion of NOAA atmospheric dry air CH4 mole fractions to a gravimetrically prepared standard scale, Journal of Geophysical Research: Atmospheres, 110, https://doi.org/10.1029/2005JD006035, https://agupubs.onlinelibrary.wiley.com/doi/abs/10.1029/2005JD006035, 2005.

Erisman, J., Sutton, M., Galloway, J., Klimont, Z., and Winiwarter, W.: How a century of ammonia synthesis changed the world, Nature Geoscience, 1, 636–639, https://doi.org/10.1038/ngeo325, http://pure.iiasa.ac.at/id/eprint/8475/, 2008.

Filges, A., Gerbig, C., Chen, H., Franke, H., Klaus, C., and Jordan, A.: The IAGOS-core greenhouse gas package: a measurement system for continuous airborne observations of CO2, CH4, H2O and CO, Tellus B: Chemical and Physical Meteorology, 67, 27 989, https://doi.org/10.3402/tellusb.v67.27989, https://doi.org/10.3402/tellusb.v67.27989, 2015.

Flechard, C., Ambus, P., Skiba, U., Rees, R., Hensen, A., van Amstel, A., van den Pol-van Dasselaar, A., Soussana, J.-F., Jones, M., Clifton-Brown, J., Raschi, A., Horvath, L., Neftel, A., Jocher, M., Ammann, C., Leifeld, J., Fuhrer, J., Calanca, P., Thalman, E., Pilegaard, K., Marco, C. D., Campbell, C., Nemitz, E., Hargreaves, K., Levy, P., Ball, B., Jones, S., van de Bulk, W., Groot, T., Blom, M., Domingues, R., Kasper, G., Allard, V., Ceschia, E., Cellier, P., Laville, P., Henault, C., Bizouard, F., Abdalla, M., Williams, M., Baronti, S., Berretti, F., and Grosz, B.: Effects of climate and management intensity on nitrous oxide emissions in grassland systems across Europe, Agriculture, Ecosystems & Environment, 121, 135 – 152, https://doi.org/https://doi.org/10.1016/j.agee.2006.12.024, http://www.sciencedirect.com/science/article/pii/S0167880906004385, the Greenhouse Gas Balance of Grasslands in Europe, 2007.

Frankenberg, C., Kulawik, S. S., Wofsy, S. C., Chevallier, F., Daube, B., Kort, E. A., O'Dell, C., Olsen, E. T., and Osterman, G.: Using airborne HIAPER Pole-to-Pole Observations (HIPPO) to evaluate model and remote sensing estimates of atmospheric carbon dioxide, Atmospheric Chemistry and Physics, 16, 7867–7878, http://proxy.lib.umich.edu/login?url=https://search-proquest-com.proxy.lib.umich.edu/docview/1803050742?accountid=14667, copyright - Copyright Copernicus GmbH 2016; Last updated - 2018-01-23, 2016.

Fried, A., Diskin, G., Weibring, P., Richter, D., Walega, J., Sachse, G., Slate, T., Rana, M., and Podolske, J.: Tunable infrared laser instruments for airborne atmospheric studies, Applied Physics B, 92, 409–417, https://doi.org/10.1007/s00340-008-3136-x, https://doi.org/10.1007/s00340-008-3136-x, 2008.

Griffis, T. J., Chen, Z., Baker, J. M., Wood, J. D., Millet, D. B., Lee, X., Venterea, R. T., and Turner, P. A.: Nitrous oxide emissions are enhanced in a warmer and wetter world, Proceedings of the National Academy of Sciences, 114, 12 081–12 085, https://doi.org/10.1073/pnas.1704552114, http://www.pnas.org/content/114/45/12081, 2017.

Hall, B. D., Dutton, G. S., and Elkins, J. W.: The NOAA nitrous oxide standard scale for atmospheric observations, Journal of Geophysical Research: Atmospheres, 112, https://doi.org/10.1029/2006JD007954, https://agupubs.onlinelibrary.wiley.com/doi/abs/10.1029/2006JD007954, 2007.

Inoue, M., Morino, I., Uchino, O., Nakatsuru, T., Yoshida, Y., Yokota, T., Wunch, D., Wennberg, P. O., Roehl, C. M., Griffith, D. W. T., Velazco, V. A., Deutscher, N. M., Warneke, T., Notholt, J., Robinson, J., Sherlock, V., Hase, F., Blumenstock, T., Rettinger, M., Sussmann, R., Kyrö, E., Kivi, R., Shiomi, K., Kawakami, S., De Mazière, M., Arnold, S. G., Feist, D. G., Barrow, E. A., Barney, J., Dubey, M., Schneider, M., Iraci, L. T., Podolske, J. R., Hillyard, P. W., Machida, T., Sawa, Y., Tsuboi, K., Matsueda, H., Sweeney, C., Tans, P. P., Andrews, A. E., Biraud, S. C., Fukuyama, Y., Pittman, J. V., Kort, E. A., and Tanaka, T.: Bias corrections of GOSAT SWIR XCO_2 and XCH_4 with TCCON data and their evaluation using aircraft measurement data, Atmospheric Measurement Techniques, 9, 3491–3512, https://doi.org/10.5194/amt-9-3491-2016, https://www.atmos-meas-tech.net/9/3491/2016/, 2016.

Karion, A., Sweeney, C., Wolter, S., Newberger, T., Chen, H., Andrews, A., Kofler, J., Neff, D., and Tans, P.: Long-term greenhouse gas measurements from aircraft, Atmospheric Measurement Techniques, 6, 511–526, https://doi.org/10.5194/amt-6-511-2013, https://www.atmos-meas-tech.net/6/511/2013/, 2013.

Karion, A., Sweeney, C., Kort, E. A., Shepson, P. B., Brewer, A., Cambaliza, M., Conley, S. A., Davis, K., Deng, A., Hardesty, M., Herndon, S. C., Lauvaux, T., Lavoie, T., Lyon, D., Newberger, T., Pétron, G., Rella, C., Smith, M., Wolter, S., Yacovitch, T. I., and Tans, P.: Aircraft-Based Estimate of Total Methane Emissions from the Barnett Shale Region, Environmental Science & Technology, 49, 8124–8131, https://doi.org/10.1021/acs.est.5b00217, https://doi.org/10.1021/acs.est.5b00217, pMID: 26148550, 2015.

Kort, E. A., Eluszkiewicz, J., Stephens, B. B., Miller, J. B., Gerbig, C., Nehrkorn, T., Daube, B. C., Kaplan, J. O., Houweling, S., and Wofsy, S. C.: Emissions of CH4 and N2O over the United States and Canada based on a receptor-oriented modeling framework and COBRA-NA atmospheric observations, Geophysical Research Letters, 35, https://doi.org/10.1029/2008GL034031, https://agupubs.onlinelibrary.wiley.com/doi/abs/10.1029/2008GL034031, 2008.

Kort, E. A., Patra, P. K., Ishijima, K., Daube, B. C., Jiménez, R., Elkin, J., Hurst, D., Moore, F. L., Sweeney, C., and Wofsy, S. C.: Tropospheric distribution and variability of N2O: Evidence for strong tropical emissions, Geophysical Research Letters, 38, https://doi.org/10.1029/2011GL047612, https://agupubs.onlinelibrary.wiley.com/doi/abs/10.1029/2011GL047612, 2011.

Kort, E. A., Smith, M. L., Murray, L. T., Gvakharia, A., Brandt, A. R., Peischl, J., Ryerson, T. B., Sweeney, C., and Travis, K.: Fugitive emissions from the Bakken shale illustrate role of shale production in global ethane shift, Geophysical Research Letters, 43, 4617–4623, https://doi.org/10.1002/2016GL068703, https://agupubs.onlinelibrary.wiley.com/doi/abs/10.1002/2016GL068703, 2016.

Lebegue, B., Schmidt, M., Ramonet, M., Wastine, B., Yver Kwok, C., Laurent, O., Belviso, S., Guemri, A., Philippon, C., Smith, J., et al.: Comparison of nitrous oxide (N 2 O) analyzers for high-precision measurements of atmospheric mole fractions, Atmospheric Measurement Techniques, 9, 1221–1238, 2016.

Marinho, E. V. A., DeLaune, R. D., and Lindau, C. W.: Nitrous Oxide Flux from Soybeans Grown on Mississippi Alluvial Soil, Communications in Soil Science and Plant Analysis, 35, 1–8, https://doi.org/10.1081/CSS-120027630, https://doi.org/10.1081/CSS-120027630, 2004.

McManus, J. B., Kebabian, P. L., and Zahniser, M. S.: Astigmatic mirror multipass absorption cells for long-path-length spectroscopy, Appl. Opt., 34, 3336–3348, https://doi.org/10.1364/AO.34.003336, http://ao.osa.org/abstract.cfm?URI=ao-34-18-3336, 1995.

Mehrotra, S., Faloona, I., Suard, M., Conley, S., and Fischer, M. L.: Airborne Methane Emission Measurements for Selected Oil and Gas Facilities Across California, Environ. Sci. Technol., 51, 12 981–12 987, 2017.

Miller, S. M., Kort, E. A., Hirsch, A. I., Dlugokencky, E. J., Andrews, A. E., Xu, X., Tian, H., Nehrkorn, T., Eluszkiewicz, J., Michalak, A. M., and Wofsy, S. C.: Regional sources of nitrous oxide over the United States: Seasonal variation and spatial distribution, Journal of Geophysical Research: Atmospheres, 117, https://doi.org/10.1029/2011JD016951, https://agupubs.onlinelibrary.wiley.com/doi/abs/10.1029/2011JD016951, 2012.

Monni, S., Perälä, P., and Regina, K.: Uncertainty in Agricultural CH4 AND N2O Emissions from Finland – Possibilities to Increase Accuracy in Emission Estimates, Mitigation and Adaptation Strategies for Global Change, 12, 545–571, https://doi.org/10.1007/s11027-006-4584-4, https://doi.org/10.1007/s11027-006-4584-4, 2007.

Myhre, G., Shindell, D., Bréon, F.-M., Collins, W., Fuglestvedt, J., Huang, J., Koch, D., Lamarque, J.-F., Lee, D., Mendoza, B., Nakajima, T., Robock, A., Stephens, G., Takemura, T., and Zhang, H.: Anthropogenic and natural radiative forcing, in: Climate Change 2013: The Physical Science Basis. Contribution of Working Group I to the Fifth Assessment Report of the Intergovernmental Panel on Climate

Change, edited by Stocker, T. F., Qin, D., Plattner, G.-K., Tignor, M., Allen, S. K., Doschung, J., Nauels, A., Xia, Y., Bex, V., and Midgley, P. M., pp. 659–740, Cambridge University Press, Cambridge, UK, https://doi.org/10.1017/CBO9781107415324.018, 2013.

Nelson, D., Shorter, J., McManus, J., and Zahniser, M.: Sub-part-per-billion detection of nitric oxide in air using a thermoelectrically cooled mid-infrared quantum cascade laser spectrometer, Applied Physics B, 75, 343–350, https://doi.org/10.1007/s00340-002-0979-4, https://doi.org/10.1007/s00340-002-0979-4, 2002.

Nelson, D. D., McManus, B., Urbanski, S., Herndon, S., and Zahniser, M. S.: High precision measurements of atmospheric nitrous oxide and methane using thermoelectrically cooled mid-infrared quantum cascade lasers and detectors, Spectrochimica Acta Part A: Molecular and Bioctroscopy, 60, 3325 – 3335, https://doi.org/https://doi.org/10.1016/j.saa.2004.01.033, http://www.sciencedirect.com/science/article/pii/S138614250400109X, 2004.

Nevison, C., Andrews, A., Thoning, K., Dlugokencky, E., Sweeney, C., Miller, S., Saikawa, E., Benmergui, J., Fischer, M., Mountain, M., and Nehrkorn, T.: Nitrous Oxide Emissions Estimated With the CarbonTracker-Lagrange North American Regional Inversion Framework, Global Biogeochemical Cycles, 32, 463–485, https://doi.org/10.1002/2017GB005759, https://agupubs.onlinelibrary.wiley.com/doi/abs/10.1002/2017GB005759, 2018.

Novelli, P. C., Masarie, K. A., Lang, P. M., Hall, B. D., Myers, R. C., and Elkins, J. W.: Reanalysis of tropospheric CO trends: Effects of the 1997-1998 wildfires, Journal of Geophysical Research (Atmospheres), 108, 4464, https://doi.org/10.1029/2002JD003031, 2003.

O'Shea, S. J., Bauguitte, S. J.-B., Gallagher, M. W., Lowry, D., and Percival, C. J.: Development of a cavity-enhanced absorption spectrometer for airborne measurements of CH_4 and CO_2, Atmospheric Measurement Techniques, 6, 1095–1109, https://doi.org/10.5194/amt-6-1095-2013, https://www.atmos-meas-tech.net/6/1095/2013/, 2013.

O'Shea, S. J., Allen, G., Gallagher, M. W., Bower, K., Illingworth, S. M., Muller, J. B. A., Jones, B. T., Percival, C. J., Bauguitte, S. J.-B., Cain, M., Warwick, N., Quiquet, A., Skiba, U., Drewer, J., Dinsmore, K., Nisbet, E. G., Lowry, D., Fisher, R. E., France, J. L., Aurela, M., Lohila, A., Hayman, G., George, C., Clark, D. B., Manning, A. J., Friend, A. D., and Pyle, J.: Methane and carbon dioxide fluxes and their regional scalability for the European Arctic wetlands during the MAMM project in summer 2012, Atmospheric Chemistry and Physics, 14, 13 159–13 174, https://doi.org/10.5194/acp-14-13159-2014, https://www.atmos-chem-phys.net/14/13159/2014/, 2014.

Pattey, E., Edwards, G., Desjardins, R., Pennock, D., Smith, W., Grant, B., and MacPherson, J.: Tools for quantifying N2O emissions from agroecosystems, Agricultural and Forest Meteorology, 142, 103 – 119, https://doi.org/https://doi.org/10.1016/j.agrformet.2006.05.013, http://www.sciencedirect.com/science/article/pii/S0168192306002899, the Contribution of Agriculture to the State of Climate, 2007.

Peischl, J., Ryerson, T. B., Aikin, K. C., Gouw, J. A., Gilman, J. B., Holloway, J. S., Lerner, B. M., Nadkarni, R., Neuman, J. A., Nowak, J. B., Trainer, M., Warneke, C., and Parrish, D. D.: Quantifying atmospheric methane emissions from the Haynesville, Fayetteville, and northeastern Marcellus shale gas production regions, Journal of Geophysical Research: Atmospheres, 120, 2119–2139, https://doi.org/10.1002/2014JD022697, https://agupubs.onlinelibrary.wiley.com/doi/abs/10.1002/2014JD022697, 2015.

Pennock, D., Farrell, R., Desjardins, R., Pattey, E., and MacPherson, J. I.: Upscaling chamber-based measurements of N2O emissions at snowmelt, Canadian Journal of Soil Science, 85, 113–125, https://doi.org/10.4141/S04-040, https://doi.org/10.4141/S04-040, 2005.

Pitt, J. R., Le Breton, M., Allen, G., Percival, C. J., Gallagher, M. W., Bauguitte, S. J.-B., O'Shea, S. J., Muller, J. B. A., Zahniser, M. S., Pyle, J., and Palmer, P. I.: The development and evaluation of airborne in situ N_2O and CH_4 sampling using a quantum cascade laser absorption spectrometer (QCLAS), Atmospheric Measurement Techniques, 9, 63–77, https://doi.org/10.5194/amt-9-63-2016, https://www.atmos-meas-tech.net/9/63/2016/, 2016.

Rannik, U., Haapanala, S., Shurpali, N. J., Mammarella, I., Lind, S., Hyvonen, N., Peltola, O., Zahniser, M., Martikainen, P. J., and Vesala, T.: Intercomparison of fast response commercial gas analysers for nitrous oxide flux measurements under field conditions, Biogeosciences, 12, 415–432, https://doi.org/10.5194/bg-12-415-2015, https://www.biogeosciences.net/12/415/2015/, 2015.

Rapson, T. D. and Dacres, H.: Analytical techniques for measuring nitrous oxide, TrAC Trends in Analytical Chemistry, 54, 65 – 74, https://doi.org/https://doi.org/10.1016/j.trac.2013.11.004, http://www.sciencedirect.com/science/article/pii/S0165993613002574, 2014.

Ravishankara, A. R., Daniel, J. S., and Portmann, R. W.: Nitrous Oxide (N2O): The Dominant Ozone-Depleting Substance Emitted in the 21st Century, Science, 326, 123–125, https://doi.org/10.1126/science.1176985, http://science.sciencemag.org/content/326/5949/123, 2009.

Rella, C. W., Chen, H., Andrews, A. E., Filges, A., Gerbig, C., Hatakka, J., Karion, A., Miles, N. L., Richardson, S. J., Steinbacher, M., Sweeney, C., Wastine, B., and Zellweger, C.: High accuracy measurements of dry mole fractions of carbon dioxide and methane in humid air, Atmospheric Measurement Techniques, 6, 837–860, https://doi.org/10.5194/amt-6-837-2013, https://www.atmos-meas-tech.net/6/837/2013/, 2013.

Rothman, L. S., Gordon, I. E., Babikov, Y., Barbe, A., Chris Benner, D., Bernath, P. F., Birk, M., Bizzocchi, L., Boudon, V., Brown, L. R., Campargue, A., Chance, K., Cohen, E. A., Coudert, L. H., Devi, V. M., Drouin, B. J., Fayt, A., Flaud, J.-M., Gamache, R. R., Harrison, J. J., Hartmann, J.-M., Hill, C., Hodges, J. T., Jacquemart, D., Jolly, A., Lamouroux, J., Le Roy, R. J., Li, G., Long, D. A., Lyulin, O. M., Mackie, C. J., Massie, S. T., Mikhailenko, S., Müller, H. S. P., Naumenko, O. V., Nikitin, A. V., Orphal, J., Perevalov, V., Perrin, A., Polovtseva, E. R., Richard, C., Smith, M. A. H., Starikova, E., Sung, K., Tashkun, S., Tennyson, J., Toon, G. C., Tyuterev, V. G., and Wagner, G.: The HITRAN2012 molecular spectroscopic database, Journal of Quantitiative Spectroscopy and Radiative Transfer, 130, 4–50, https://doi.org/10.1016/j.jqsrt.2013.07.002, 2013.

Ruser, R., Flessa, H., Russow, R., Schmidt, G., Buegger, F., and Munch, J.: Emission of N2O, N2 and CO2 from soil fertilized with nitrate: effect of compaction, soil moisture and rewetting, Soil Biology and Biochemistry, 38, 263 – 274, https://doi.org/https://doi.org/10.1016/j.soilbio.2005.05.005, http://www.sciencedirect.com/science/article/pii/S0038071705001975, 2006.

Santoni, G. W., Daube, B. C., Kort, E. A., Jiménez, R., Park, S., Pittman, J. V., Gottlieb, E., Xiang, B., Zahniser, M. S., Nelson, D. D., McManus, J. B., Peischl, J., Ryerson, T. B., Holloway, J. S., Andrews, A. E., Sweeney, C., Hall, B., Hintsa, E. J., Moore, F. L., Elkins, J. W., Hurst, D. F., Stephens, B. B., Bent, J., and Wofsy, S. C.: Evaluation of the airborne quantum cascade laser spectrometer (QCLS) measurements of the carbon and greenhouse gas suite - CO_2, CH_4, N_2O, and CO - during the CalNex and HIPPO campaigns, Atmospheric Measurement Techniques, 7, 1509–1526, https://doi.org/10.5194/amt-7-1509-2014, https://www.atmos-meas-tech.net/7/1509/2014/, 2014.

Smith, M. L., Kort, E. A., Karion, A., Sweeney, C., Herndon, S. C., and Yacovitch, T. I.: Airborne Ethane Observations in the Barnett Shale: Quantification of Ethane Flux and Attribution of Methane Emissions, Environmental Science & Technology, 49, 8158–8166, https://doi.org/10.1021/acs.est.5b00219, https://doi.org/10.1021/acs.est.5b00219, pMID: 26148554, 2015.

Tanaka, T., Yates, E., Iraci, L. T., Johnson, M. S., Gore, W., Tadić, J. M., Loewenstein, M., Kuze, A., Frankenberg, C., Butz, A., and Yoshida, Y.: Two-Year Comparison of Airborne Measurements of CO2 and CH4 With GOSAT at Railroad Valley, Nevada, IEEE Transactions on Geoscience and Remote Sensing, 54, 4367–4375, 2016.

Tans, P. P., Crotwell, A. M., and Thoning, K. W.: Abundances of isotopologues and calibration of CO_2 greenhouse gas measurements, Atmospheric Measurement Techniques, 10, 2669–2685, https://doi.org/10.5194/amt-10-2669-2017, https://www.atmos-meas-tech.net/10/2669/2017/, 2017.

Thompson, R. L., Chevallier, F., Crotwell, A. M., Dutton, G., Langenfelds, R. L., Prinn, R. G., Weiss, R. F., Tohjima, Y., Nakazawa, T., Krummel, P. B., Steele, L. P., Fraser, P., O'Doherty, S., Ishijima, K., and Aoki, S.: Nitrous oxide emissions 1999 to 2009 from

a global atmospheric inversion, Atmospheric Chemistry and Physics, 14, 1801–1817, https://doi.org/10.5194/acp-14-1801-2014, https://www.atmos-chem-phys.net/14/1801/2014/, 2014.

Tian, H., Chen, G., Lu, C., Xu, X., Ren, W., Zhang, B., Banger, K., Tao, B., Pan, S., Liu, M., Zhang, C., Bruhwiler, L., and Wofsy, S.: Global methane and nitrous oxide emissions from terrestrial ecosystems due to multiple environmental changes, Ecosystem Health and Sustainability, 1, 1–20, https://doi.org/10.1890/EHS14-0015.1, https://esajournals.onlinelibrary.wiley.com/doi/abs/10.1890/EHS14-0015.1, 2015.

Turner, D. A., Chen, D., Galbally, I. E., Leuning, R., Edis, R. B., Li, Y., Kelly, K., and Phillips, F.: Spatial variability of nitrous oxide emissions from an Australian irrigated dairy pasture, Plant and Soil, 309, 77–88, https://doi.org/10.1007/s11104-008-9639-8, https://doi.org/10.1007/s11104-008-9639-8, 2008.

Vaughn, T. L., Bell, C. S., Yacovitch, T. I., Roscioli, J. R., Herndon, S. C., Conley, S., Schwietzke, S., Heath, G. A., Pétron, G., and Zimmerle, D.: Comparing facility-level methane emission rate estimates at natural gas gathering and boosting stations, Elem Sci Anth, 5, 71, https://doi.org/10.1525/elementa.257, https://doi.org/10.1525/elementa.257, 2017.

WMO, W.: 18th WMO/IAEA Meeting on Carbon Dioxide, Other Greenhouse Gases and Related Tracers Measurement Techniques (GGMT-2015), GAW Report- No. 229, 2015.

Wofsy, S. C.: HIAPER Pole-to-Pole Observations (HIPPO): fine-grained, global-scale measurements of climatically important atmospheric gases and aerosols, Philosophical Transactions of the Royal Society of London A: Mathematical, Physical and Engineering Sciences, 369, 2073–2086, https://doi.org/10.1098/rsta.2010.0313, http://rsta.royalsocietypublishing.org/content/369/1943/2073, 2011.

Xiang, B., Miller, S. M., Kort, E. A., Santoni, G. W., Daube, B. C., Commane, R., Angevine, W. M., Ryerson, T. B., Trainer, M. K., Andrews, A. E., Nehrkorn, T., Tian, H., and Wofsy, S. C.: Nitrous oxide (N2O) emissions from California based on 2010 CalNex airborne measurements, Journal of Geophysical Research: Atmospheres, 118, 2809–2820, https://doi.org/10.1002/jgrd.50189, https://agupubs.onlinelibrary.wiley.com/doi/abs/10.1002/jgrd.50189, 2013.

Yacovitch, T. I., Herndon, S. C., Roscioli, J. R., Floerchinger, C., McGovern, R. M., Agnese, M., Pétron, G., Kofler, J., Sweeney, C., Karion, A., Conley, S. A., Kort, E. A., Nähle, L., Fischer, M., Hildebrandt, L., Koeth, J., McManus, J. B., Nelson, D. D., Zahniser, M. S., and Kolb, C. E.: Demonstration of an Ethane Spectrometer for Methane Source Identification, Environmental Science & Technology, 48, 8028–8034, https://doi.org/10.1021/es501475q, http://dx.doi.org/10.1021/es501475q, pMID: 24945706, 2014.

Zhao, C. L. and Tans, P. P.: Estimating uncertainty of the WMO mole fraction scale for carbon dioxide in air, Journal of Geophysical Research: Atmospheres, 111, https://doi.org/10.1029/2005JD006003, https://agupubs.onlinelibrary.wiley.com/doi/abs/10.1029/2005JD006003, 2006.

Zhao, C. L., Tans, P. P., and Thoning, K. W.: A high precision manometric system for absolute calibrations of CO2 in dry air, Journal of Geophysical Research: Atmospheres, 102, 5885–5894, https://doi.org/10.1029/96JD03764, https://agupubs.onlinelibrary.wiley.com/doi/abs/10.1029/96JD03764, 1997.